Journal of Inclusion Phenomena and Molecular Recognition in Chemistry **21**: 1–46, 1995.

Probing Intrazeolite Space

LLOYD ABRAMS and DAVID R. CORBIN

1. Introduction

Molecular sieves are crystalline materials with open framework structures. Of the almost two billion pounds of molecular sieves produced in 1990, 1.4 billion pounds were used in detergents, 160 million pounds as catalysts, and about 70 million pounds as adsorbents or desiccants [1]. Zeolites, composed of aluminosilicates, represent a large fraction of known molecular sieves. The primary building blocks of zeolites are $[SiO_4]^{4-}$ and $[AlO_4]^{5-}$ tetrahedra which are linked by their corners to form channels and cages or cavities of discrete size The pore openings to these channels and cages generally range from about 3 to 20 Å. As a result of the difference in charge between the $[SiO_4]^{4-}$ and $[AlO_4]^{5-}$ tetrahedra, the total framework charge of an aluminum-containing molecular sieve is negative and hence must be balanced by cations, typically protons, alkali, or alkaline earth metal ions.

Over 500 materials are listed in the *Handbook of Molecular Sieves* including at least 40 naturally occurring zeolites [2]. The numerous framework topologies of the molecular sieves offer various systems of channels and cavities resulting in one-, two-, or three-dimensional diffusion for included guest molecules. For example, so-called one-dimensional molecular sieves have channels parallel to one another and there are no connecting channels large enough for guest molecules to cross from one channel to the next.

The variety in structure types provides a range of pore dimensions from the small-pore materials consisting of ring openings containing eight of the tetrahedra, to the medium-pore zeolites with 10-membered ring openings, and the large-pore materials with 12-membered ring openings. Larger pore openings have been reported for the aluminum phosphate molecular sieves, such as $AlPO_4$-8, VPI-5 with 14- and 18-membered rings, respectively, and cloverite, a $GaPO_4$ with 20-membered rings [3]. For the same number of ring members, variations in pore geometry, for example, elliptical vs. circular, can have a marked effect on sorption properties especially when the openings are similar in size to the sorbing molecules.

Molecular sieves can be characterized not only by their channel systems but, in many cases, also by the polyhedral cavities or cages present. The aluminosilicate backbone of a zeolite molecular sieve can be represented in a number of ways which are illustrated in Figure 1 for the beta- or sodalite-cage.

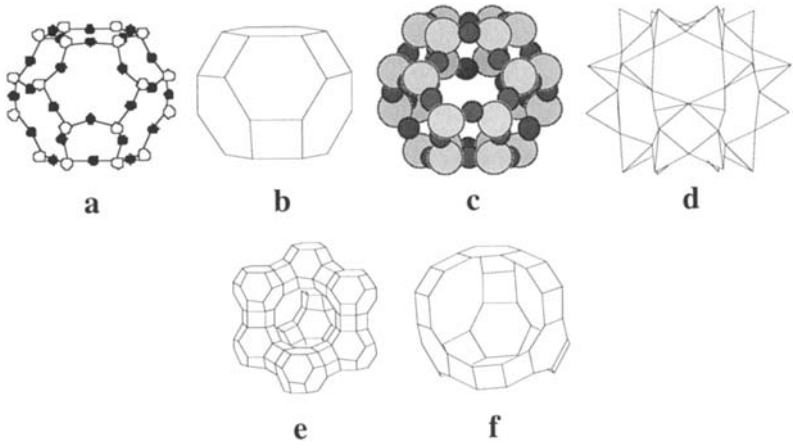

Figure 1. Representations (a-d) of the structures of the sodalite cage [using (a) a 'ball and stick' model; (b) a 'tetrahedral array' in which 'single bonds' join the framework **T** (T = Si, Al) atoms (The bridging oxygen atoms are not shown for simplicity); (c) 'space-filling' model; and (d) 'tetrahedral presentation' showing the arrangement of framework tetrahedra]; (e) faujasite ('tetrahedral array' with bridging oxygens removed); and (f) the supercage ('tetrahedral array' with bridging oxygens removed).

The sodalite cage structure is constructed of openings containing 4- and 6-membered rings of $[SiO_4]^{4-}$ and $[AlO_4]^{5-}$ tetrahedra. (In the literature, TO_2 (T = Si, Al) is also used to represent the framework tetrahedra [4].) The faujasite structure (see Figure 1) is constructed of sodalite cages connected through oxygen bridges at the 6-rings and the largest pore opening is a 12-membered ring. The sodalite cages surround an even larger cage, the supercage, which forms a three-dimensional network with each supercage connected tetrahedrally to four other supercages through the 12-membered ring opening.

In order to quantify the amount of molecular sieve in a sample and to understand and predict packing, sieving, and migration effects of absorbed molecules, the sizes of the framework constituents and internal void geometry must be known with a high degree of precision. Neutron diffraction provides excellent structural resolution but is not a common laboratory tool. Therefore, structures of molecular sieves are generally derived from X-ray diffraction patterns of powders because large single-crystals are not available (most molecular sieve preparations yield particles in the micron size range). The exact

size and shape of the internal structures are, at best, only approximated by the X-ray technique because:

- different framework atoms (e.g., silicon and aluminum) are not readily distinguished nor is their siting necessarily identical from unit cell to unit cell.
- the location of charge compensating ions (especially protons) is difficult to identify.
- the size of the framework oxygen must be estimated.

Furthermore, the presence of small amounts of other phases and/or inclusions within the framework may not be detected or quantified. However, it is essential to have a good measure of the pore opening, channel, and cage dimensions of molecular sieves in order to describe:

- the ability to differentially absorb molecules on the basis of size (sieving ability).
- the rates of migration of molecules into and within the structures.
- the packing of molecules absorbed within the framework.

As noted above, the precise location of active sites, ions, and occlusions within the frameworks may not be known. Without detailed measurements of these factors, it is difficult to predict the chemical reaction selectivity imposed by framework structures. Sorption measurements using molecular probes of appropriate size, geometry, and chemistry can help provide such a description. Such measurements are relied upon to provide information about the framework dimensions, i.e., size and shape selectivity, as well as accessible framework volumes. For example, Na-A zeolite does not absorb molecules larger than 3.6 Å at 77 K, while at 300 K it will absorb molecules of 4.0 Å in diameter [5]. Such a change in channel dimensions with temperature is much larger than would be inferred from coefficient of expansion data but re-siting (migration) of the Na ion from the 8-ring to the cage would permit such absorption. As such, absorption measurements provide a good description of effective channel dimensions which is essential if inferences are going to be made concerning diffusion of molecules within framework structures and chemical reaction selectivity imposed by those structures.

This chapter will focus primarily on the authors' studies on zeolites A, rho, and ZSM-5 using physical sorption measurements in conjunction with X-ray diffraction. The authors will use the term "adsorption" to include all sorption phenomena involving sorption on external particle or crystal surfaces and will reserve the term "absorption" for use in describing sorption inside the frameworks. The amount adsorbed can be distinguished from the absorbed amount (*vide infra*). This chapter is not intended to be all-inclusive regarding sorption phenomena but to provide the reader with important concepts and the basis for characterizing other framework structures. Other techniques, such as chemisorption, IR, NMR, etc. will be discussed somewhat in other chapters or in other monographs [6]. Here, the utility of adsorption measurements will be demonstrated to show that a given framework dictates the equilibrium sorption values depending upon the sorbates' size and geometry. By using X-ray diffraction coupled with adsorption measurements, a good estimation of the accessible (available for absorption) framework can be made; in some cases, this capability permits the crystallinity of a sample to be determined.

2. Considerations

As noted above, when X-ray diffraction analysis is applied to framework structures there are some limitations compared to its application on dense crystalline solids. The unit cells of molecular sieves are often larger and the diffraction patterns have many more lines. Small amounts of impurity phases are virtually invisible but they can have pronounced effects on a sample's absorption properties. In order to fully understand the dimensions controlling absorption and filling of frameworks, the size of the framework oxygen must be defined. Once having established how oxygen is bound to other framework species, other factors become important. Filling of the framework and the estimation of pore volume, the packing of the absorbed molecules, estimation of the amount adsorbed on the external crystal surfaces versus the amount absorbed into the framework, the choice of molecules to probe the framework, and what experimental difficulties typically befall the experimentalist will be addressed in this section.

2.1 SIZE OF OXYGEN

A dilemma exists in the field concerning the usage of X-ray diffraction and absorption of molecules, that is, in making the "correct" choice of sizes that describe both the molecular sieve and sorbate dimensions. For the ideal planar configuration illustrated in Figure 2, the O-O interatomic distance across the 8-membered ring would be 6.9 Å. With the

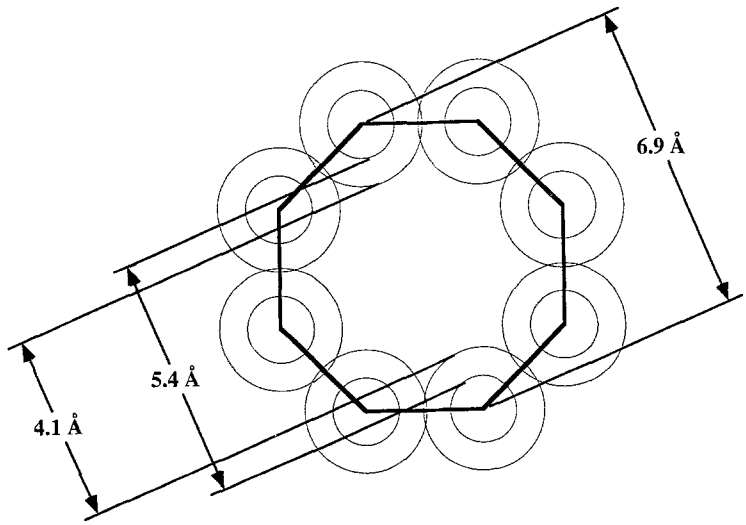

Figure 2. An ideal planar configuration of an 8-membered ring system showing the effect of oxygen ionicity on the pore opening dimension.

Table 1. The ideal planar pore: the dependency of size on oxygen ionicity.

Number of T Atoms in Ring#	Interatomic Distance Å	Circular Pore Opening Distance	
		Ionic O† Å	Covalent O† Å
4	3.71	0.96	2.21
5	4.03	1.69	2.95
6	4.46	1.71	2.96
8	6.86	4.11	5.36
10	8.55	5.80	7.05
12	10.21	7.46	8.71
14	11.89	9.14	10.39
18	15.21	12.46	13.71
20	16.87	14.12	15.37

† A diameter of 2.7 Å is used for ionic oxygen [7]; a diameter of 1.5 Å for covalent oxygen [7].

Number of tetrahedra forming the pore.

framework T (Si, Al) and O atoms fixed, the size of the oxygen atoms will determine the size of the pore opening. If the framework oxygen were ionic in character, its diameter would be 2.7 Å [8] and the opening of the ring would be 4.1 Å. If the oxygen were purely covalent, the ring opening would be 5.4 Å. As shown in Table 1, the openings can vary significantly depending upon the ionicity of the framework oxygen.

The assumption that the framework oxygen is ionic (i.e., 2.7 Å diameter) has been made so often that the literature has many examples of apparent contradictions: for example, molecules almost 5 Å in size (e.g., isopropanol, trimethylamine) sorb into 8-ring structures such as zeolites A and rho, although the ring openings are cited as 3.6 Å and 4.1 Å, respectively [7]. There appears to be ample evidence that the framework oxygen is more covalently bound to silicon such that its size is closer to 1.5 Å (probably ~ 1.7 Å). Furthermore, ZSM-5 zeolites are generally hydrophobic which is difficult to rationalize in terms of highly ionic framework oxygen. The amount of water sorbed by ZSM-5 depends directly on the aluminum content of the framework [9] but the amount of hexane sorbed is independent. ZSM-5 is typical of the 10-membered ring systems which readily absorb benzene which is listed as having a width of 6.6 Å (Pauling) [5]; this dimension is larger than the ring opening of 5.8 Å based on the crystal structure and using the diameter of ionic oxygen. Other investigators have addressed the problem of assigning the appropriate molecular dimensions [10]. Dimensions used in this chapter were obtained from molecular models, Fisher-Hirschfelder-Taylor [11], which seem to provide a consistent basis for comparison of liquid density, molecular cross-sections for estimating kinetic diameters, and molecular sieving effects. From these models, Table 2 was developed and presents a summary of the dimensions of the probe molecules cited in this chapter.

Table 2. Approximate dimensions of probe molecules and abbreviations used in the text.

Molecule	Dimensions, Å [11]	Molecule	Dimensions, Å [11]
nitrogen, N_2	2.6x2.6x3.8	i-propanol, iPOH	4.6x5.0x6.1
water, H_2O	2.6x2.8x3.6	*m*-xylene, mxyl	3.6x7.2x8.6
methanol, MeOH	3.6x3.9x4.4	*p*-xylene, pxyl	3.6x6.5x8.9
ethanol, EtOH	3.9x4.2x6.0	*o*-xylene, oxyl	3.6x7.1x8.1
n-propanol, nPOH	3.9x4.3x7.5	3-methylpentane, 3MeP	5.1x5.9x8.0
n-hexane, nHex	3.9x4.3x9.7	toluene, tol	3.6x6.5x8.1
xenon, Xe	4.0	benzene, bz	2.5x6.5x7.2
carbon tetrachloride, CCl_4	5.4	cyclohexane, 0Hex	5.1x6.0x6.5
monomethylamine, MMA	3.7x3.9x4.4	2,2-dimethylpropane, neopentane	5.5x5.8x6.2
dimethylamine, DMA	3.9x4.7x6.0	trimethylamine, TMA	3.9x5.4x6.1

The different molecular sieve structures have slightly different sizes and shapes from the 'ideal' circular values listed in Table 1. For the various framework structures discussed in this chapter, Table 3a shows their pore and channel dimensions, "ionic" compared to "covalent" oxygen, and lists examples of those structures. Table 3b lists similar data for the more common cage structures.

2.2 ISOTHERMS AND THE LIQUID STATE

Molecular sieves yield Type I (BET) adsorption isotherms or the so-called Langmuir adsorption isotherm; characteristics of this isotherm are a steep rise in absorbed amount at low pressures and an almost constant absorbed value at high pressures. Recall that an isotherm is equilibrium adsorption data as a function of vapor pressure at a constant temperature. Since it is equilibrium data, it can and should provide thermodynamic values. At present, there is no good theoretical treatment developed that completely predicts the absorption isotherm in microporous materials such as molecular sieves.

For the most part, a molecular sieve will be filled in the relative pressure range of 0.1-0.5. In essence, filling of a molecular sieve stops the major sorption process and provides the distinctive isotherm shape. Generally, the Gurvitsch Rule governs the sorption of species into zeolites: "the uptake at saturation of different sorbates on the same adsorbent is nearly equal if expressed as the volume of liquid at the temperature of sorption" [12].

But the Gurvitsch Rule may not always be true, for example,

- when equilibrium has not been reached.
- in the temperature region near or above the homogeneous liquid's critical point.
- when steric constraints are operating.

Table 3a. Oxygen ionicity, its effect on pore and channel dimensions.

Framework Code	T atoms	Ionic Oxygen [7]	Covalent Oxygen [8]	Examples
RHO	8	3.6	4.8	rho
CHA	8	3.8	5.0	chabazite
KFI	8	3.9	5.1	ZK-5
LTA	8	4.1	5.3	A
ERI	8	3.6x5.1	4.8x6.3	erionite
MEL	10	5.3x5.4	6.5x6.6	ZSM-11, silicalite-2
MFI	10	5.3x5.6	6.5x6.8	ZSM-5, silicalite
	10	5.1x5.5	6.3x6.7	
FER	10	4.2x5.4	5.4x6.6	ferrierite
	8	3.5x4.8	4.7x6.0	
HEU	10	3.0x7.6	5.2x8.8	clinoptilolite
	8	3.3x4.6	4.5x5.8	
	6	2.6x4.7	3.8x5.9	
FAU	12	7.4	8.6	X, Y
BEA	12	7.6x6.4	8.8x7.6	beta
	10	5.5	6.7	
GME	12	7.0	8.2	gmelinite
	8	3.6x3.9	4.8x5.1	
LTL	12	7.1	8.3	L
MAZ	12	7.4	8.6	mazzite, omega
MOR	12	6.5x7.0	7.7x8.2	mordenite
	8	2.6x5.7	3.8x6.9	
OFF	12	6.7	7.9	offretite
	8	3.6x4.9	4.8x6.2	
AET	14	7.9x8.7	9.1x9.9	$AlPO_4$-8
VFI	18	12.1	13.3	VPI-5

The difficulty in dealing with absorption of vapors into microporous sorbents is that equilibration times are much longer, in general, than for adsorption on planar substrates. Instead of times on the order of seconds or minutes, the units are hours, days, and months. The problem is akin to the parking of cars in a large department store's parking lot on the day of a sale. At the early stage, there are many available spaces and parking is easy (equilibrium is reasonably rapid). During the peak of the sale, vacancy diffusion operates (a driver must wait for a space or diffusion path to open); equilibration times are long. Too often, researchers do not wait long enough to assure equilibrium, report rate phenomena on poorly characterized samples, or do not provide a large enough statistical base for interpretation of their measurements. In this chapter, we provide some

Table 3b. Oxygen ionicity, its effect on cage dimensions.

Cage or Polyhedral Building Unit[a] / Common Name(s)	Approximate Free Dimensions (Å)		Approximate Free Volume (Å^3)[b]	Zeolite Examples
	Ionic	Covalent		
$[4^6 6^2]$/D6R	1.1[c]	2.3[c]	5	FAU, KFI, CHA, ERI, OFF
$[4^8 8^2]$/D8R, Delta	3.3[d]	4.5[d]	31	RHO
$[4^6 6^5]$/Epsilon	2.3x3.5	3.5x4.7	24	ERI
$[4^6 6^8]$/Sodalite, Beta	5.4[e]	6.6[e]	151	SOD, FAU, LTA
$[4^9 6^2 8^3]$	4.8x6.2	6.0x7.4	157	GME, OFF, MAZ
$[4^{12} 8^6]$/Gamma	5.4x9.6	6.6x10.8	264	KFI
$[6^2 8^6]$	5.4x9.8	6.5x11	401	CHA
$[4^{12} 6^5 8^6]$	5.1x13.8	6.3x15	445	ERI
$[4^{12} 6^8 8^6]$Alpha	10.4[f]	11.6[f]	811[g]	LTA, KFI, RHO
$[4^{18} 6^4 12^4]$/Supercage	10.8[e]	12.0[e]	896	FAU

a. e.g., $[4^6 6^2]$ cage contains 6 four-membered rings and 2 six-membered rings.
b. Calculations of polyhedral volumes were performed using a modification of the POLYVOL program [D. K. Swanson and R. C. Peterson, "POLYVOL Program Documentation", Virginia Polytechnic Institute, Blacksburg, VA] assuming the radius of the TO_2 unit to be 2.08 Å (equivalent to that of quartz).
c. in plane of 6-ring.
d. in plane of 8-ring.
e. diameter of inscribed sphere.
f. diameter of inscribed sphere for LTA.
g. 811 Å^3 for LTA, 707 Å^3 for KFI, and 722 Å^3 for RHO.

guidance concerning these issues. Considerations of sorption phenomena in molecular sieves and microporous substrates have produced an extensive literature [13]. The references cited are not intended to provide a comprehensive bibliography on sorption in microporous substrates but were chosen to provide a reasonable starting point. The last words on sorption phenomena in molecular sieves have obviously not been written; a general treatment has not been developed to completely describe both sorption and diffusion. In order to completely describe sorption phenomena in micropores, it is essential that kinetic and equilibrium theories be compatible.

Experimental correlations are relied upon to describe molecular packing and diffusion within molecular sieves. For example, Moore and Katzer showed that a 0.4 Å difference (in molecular sieve pore versus sorbed molecule dimension) produces an order of magnitude change in effective diffusion coefficient [14]. Thus, for sorption rates of differently sized molecules into similar zeolites (for example, different preparations), rate differences relate to small differences (~0.1 Å) in channel dimensions. As such, sorption

rate measurements are very sensitive to inclusions, ions, lattice defects, framework distortions, etc. which might not otherwise be detected by other analytical techniques.

The classical Kelvin Equation, used in physical adsorption to relate the vapor pressure of a solvent to the diameter of the filled pores, is not strictly valid for the region below ~20 Å. Below this size, the macroscopic properties used in the equation are not necessarily continuous nor well-defined. Typical of the sort of problems encountered when dealing with molecular sieve dimensions is the relationship of liquid density to critical temperature. Normally, the density of a liquid decreases as the temperature increases; an increase in pressure is needed to maintain the species in the liquid state. Near the critical point, the kinetic energy term overwhelms the interactive forces of the molecules and the species can no longer be liquefied.

But the situation is quite different inside molecular sieves. The absorbed molecules, in addition to their own interactive forces, are attracted by the framework - an interaction that might be much larger than the intermolecular forces of the liquid state. Well below the critical point, if there are no constraints upon packing, the sorbed state generally packs according to the liquid's density following the Gurvitsch Rule. Shown in Figure 3, the density of ammonia in the liquid state is compared to the density of ammonia absorbed by zeolite rho. The sorption data for ammonia were taken using a microbalance at an ammonia pressure of 0.3 atm. The weight of the ammonia absorbed was measured directly while the sorption volume for zeolite rho was determined from X-ray diffraction and other absorption measurements. For the liquid state, as the temperature is increased, the pressure on the ammonia must be increased to keep it liquefied. At the critical point (T_c = 405.51 K, P_c = 111.3 atm, ρ_c = 0.235 g/cm^3), the liquid density drops precipitously.

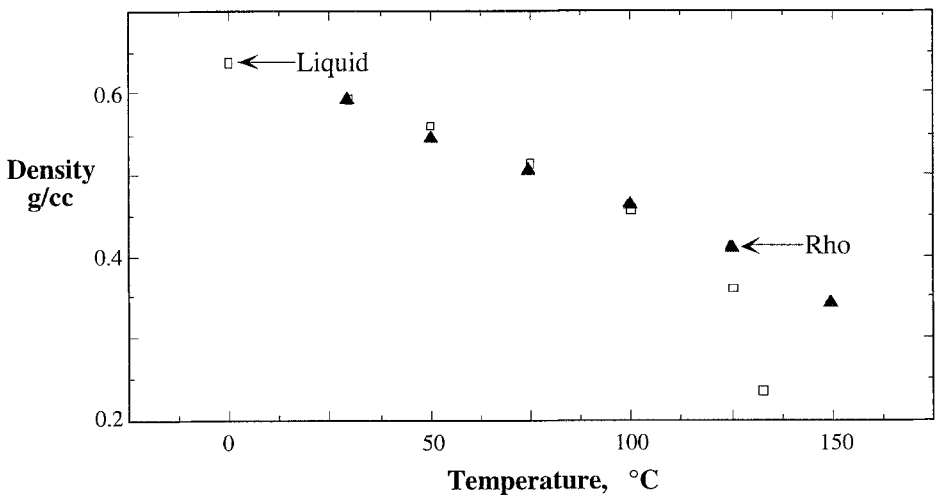

Figure 3. Effect of temperature on density of ammonia in the liquid state compared to the density of ammonia absorbed by zeolite rho.

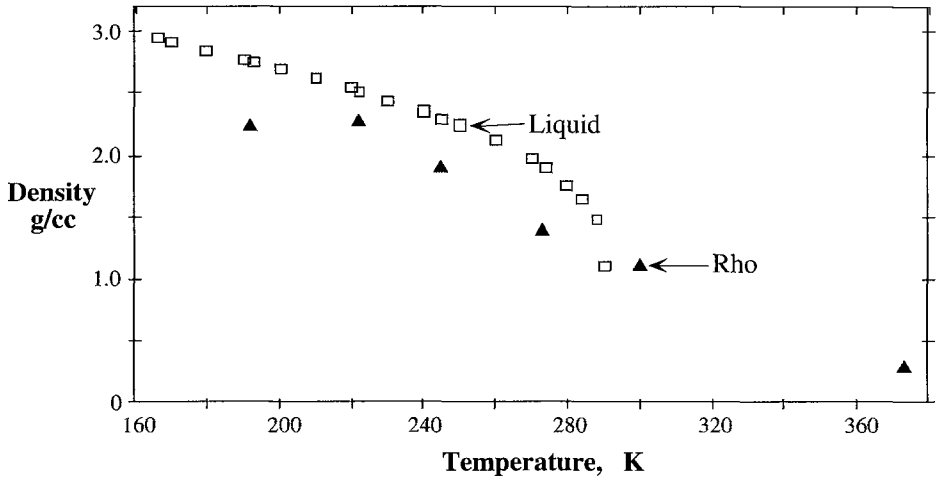

Figure 4. Effect of temperature on density of xenon in the liquid state compared to the density of xenon absorbed by zeolite rho.

However, the sorbed case shows quite different behavior: well-below the critical point, the absorbed state packs according to the liquid density even though the applied pressure may be a small fraction of that needed for the homogeneous liquid case. This behavior is termed, by us, the 'unconstrained case'. As the temperature increases and passes through the liquid's critical point, the density of the absorbed state continues to drop modestly compared to the precipitous drop in density for the homogeneous liquid. Near or above the critical point, the density-temperature plot shown in Figure 3 is typical for the behaviors of the homogeneous liquid vs. the absorbed state. At present, there is no good theory to describe the absorbed state behavior and so the packing density in micropores for a liquid near or above its critical point must be measured.

Shown in Figure 4 is the density of xenon (T_c = 289.75 K, P_c = 58.0 atm, ρ_c = 1.105 g/cm^3) in the liquid state and absorbed in zeolite rho. This Figure illustrates the case when steric constraints operate on the absorbed phase. Here, the large size of xenon coupled with the geometry and size of the cage of zeolite rho prohibits xenon from packing as a liquid at any temperature. However, the fall-off in density vs. increase in temperature of the absorbed state for the 'constrained case' is similar to the density-temperature fall-off for the unconstrained case as shown for ammonia.

2.3 EXPERIMENTAL DETAILS

Gravimetric measurements were used to follow the sorption of liquid vapors by molecular sieves. A sample cell employing a greaseless vacuum stopcock and an 'O-ring' seal was designed to contain the powders and fit on an analytical balance. Details of the activation procedure and measuring protocol were published previously [15]. Typically, samples were heated at 425° C until the pressure above the samples was $< 2x10^{-5}$ torr. If the samples' outgassing rate was < 0.1 mtorr/min at 425° C, the samples were cooled under vacuum and weighed. If the outgassing criteria were not met, sorption weights were obtained 10-25% below expectations. It typically takes 2-4 days of heating at 425° C under vacuum to prepare small-pore zeolites for sorption studies whereas it takes < 1 day for ZSM-5 zeolites to meet the outgassing criteria. The weight of powder dried in this fashion was used to calculate the amount sorbed per gram of sample. Generally, the same samples were used for a series of absorptions and desorptions. Sample weights were monitored and an oxygen burn-off was used if there was any measurable build-up. X-Ray diffraction was used to detect gross crystallinity changes.

The initial weight loss upon activation at 425° C is recorded; water desorption generally accounts for this loss. If the sample has a low external surface area, then this weight loss may provide a measure of the framework sorption capacity.

In general, two weighings, at 3 and 20 hours, were taken routinely and the ratio of amounts is called the 'Rate of Filling Ratio'. When sorption was slow or the weight gain negligible, the duration of exposure was increased. Measurements at 3 and 20 h show:

- when the framework is completely filled. If the sorption amounts are > 10 wt % and virtually equal, then the absorbing molecules are smaller than the limiting channel dimension.
- that the molecules cannot enter the framework and only occupy the exterior surface. Again, the weight gains at 3 and 20 hours are equal but are generally < 2% for this case. Longer sorption times are then used to check this point.
- that migration of the sorbing molecule is restricted by a framework dimension. In this case, the 3 hour weight gain is approximately 10-75% of the 20 hour weight gain. By changing the size and/or shape of the sorbing molecule and using Moore and Katzer's correlation, an estimate of the limiting framework dimension(s) can be made. Again, if the weight gains are low, 2-5%, the duration of the sorption process can be extended.

Most of the sorptions were performed at room temperature, 20-25° C, because they were relatively easy to do and the possibility of reaction was reduced. Sorptions at higher temperatures could be done with some additional effort but, as the system could not be analyzed during sorption at higher temperatures and the possibility of reaction increased, such measurements were postponed until suitable instrumentation would be available.

2.4 ADSORPTION (EXTERNAL SURFACE) VS. ABSORPTION (INTERNAL FRAMEWORK)

Because many molecular sieves are synthesized as micron or submicron crystals, a significant contribution to the sorbed amount could be made by the external surface. Although the BET method is synonymous with the measurement of surface area, it provides an ambiguous result when applied to molecular sieves. In general, nitrogen is used as the BET probe molecule and, at liquid nitrogen temperature, it could condense within the sieve framework. For large pore zeolites, such condensation provides an estimate of the framework pore volume. This value would have to be corrected for adsorption on the exterior surface of the crystals. For small pore zeolites, nitrogen may not be able to enter the framework such that a real measure of the external surface area can be obtained. It is desirable to be able to measure both the external surface area as well as the internal pore volume of zeolite preparations. The measured external surface area can then be used to obtain the amount adsorbed on the external surface of a zeolite powder. Using mercury porosimetry, a method was developed to estimate the amount adsorbed on the surface of the particles [16]. The amount absorbed into the framework is obtained by subtracting this surface contribution from the total weight gain. All values reported in this chapter have been corrected in this manner.

2.5 ESTIMATION OF THE FRAMEWORK PORE VOLUME

Comparison of the absorption of molecules into molecular sieves versus their adsorption on planar substrates is similar to the filling of a pail versus pouring the same amount of water on a floor. A pail will hold a finite volume of liquid while the depth of water on your basement floor depends on how quickly a plumber can get to your residence. For molecular sieves, a method is needed to estimate the internal pore volume available for absorption. By using this volume in combination with sorption data, the framework crystallinity of a sample can be calculated. The steps to do this calculation are straight-forward:

- from Avogadro's Number and the molecular weight of the empty, dehydrated molecular sieve, the number of unit cells per gram can be calculated.
- X-ray diffraction provides the dimensions of a unit cell and indicates if other species (amorphous or crystalline) are present to any large extent.
- assume that each TO_2 (SiO_2 or AlO_2^-) group in a molecular sieve occupies the same volume as in quartz (~37.6Å^3). Subtracting the volume of the TO_2 groups from the unit cell volume yields the total pore volume in a unit cell. Note: the volume of charge compensating cations as well as the volume of framework sections that may be inaccessible for adsorption (for example, the ß- or sodalite cages) can be subtracted from the total pore volume to give the accessible pore volume. Dividing the accessible pore volume per unit cell by the unit cell volume yields the Void Fraction.

- finally, determine the volume of a gram of unit cells and multiply it by the Void Fraction to give the accessible framework pore volume. Typical values will range from 0.2-0.5 cc/g; zeolites are not only molecular sieves, they are also molecular sponges.

A listing of the calculated pore volumes for a variety of zeolites is given as Table 4. Some zeolites are listed twice to show how ions or inaccessible regions, for example the ß-cage, affect the pore volume calculation.

2.6 PACKING CONSIDERATIONS AND CHOICE OF PROBE MOLECULES

From equilibrium absorption data, we can get some idea of how molecules pack into a molecular sieve framework by using solvent molecules of different dimensions. For example, if two substances pack into a molecular sieve according to their liquid densities (at temperatures well-below their critical points), then the ratio of their absorbed weights

Table 4. Calculated sorption parameters from X-ray diffraction unit cell dimensions¥.

Zeolite	Formula	UC x10^{20}	UC_V Å^3	V_f cc/cc	V cc/g	ρ g/cc	V_p cc/g
H-Rho	$H_{12}Al_{12}Si_{36}O_{96}$	2.09	3375	0.465	0.705	1.418	0.328
H,Cs-Rho	$CsH_9Al_{10}Si_{38}O_{96}$	2.01	3375	0.465	0.675	1.481	0.308
H-ZK-5	$H_{30}Al_{30}Si_{66}O_{192}$	1.04	6539	0.448	0.681	1.468	0.305
H-Chabazite	$H_4Al_4Si_8O_{24}$	8.33	822	0.451	0.685	1.460	0.309
Ca-Chabazite	$Ca_2Al_4Si_8O_{24}$	7.54	822	0.442	0.620	1.614	0.274
Na-A	$Na_{12}Al_{12}Si_{12}O_{48}$	3.52	1870	0.491	0.659	1.519	0.323
Na-A	ß-cage blocked						0.270
Ca-A	$Ca_6Al_{12}Si_{12}O_{48}$	3.60	1870	0.504	0.673	1.487	0.339
Ca-A	ß-cage blocked						0.285
H-ZK-4	$H_9Al_9Si_{15}O_{48}$	4.17	1798	0.498	0.749	1.335	0.373
H-Erionite	$H_9Al_9Si_{27}O_{72}$	2.78	2300	0.411	0.639	1.565	0.263
Ca-Erionite	$Ca_{4.5}Al_9Si_{27}O_{72}$	2.58	2300	0.403	0.592	1.689	0.239
H-Ferrierite	$H_{5.5}Al_{5.5}Si_{30.5}O_{72}$	2.78	2027	0.332	0.563	1.776	0.187
H-ZSM-5	$H_2Al_2Si_{94}O_{192}$	1.04	5500	0.344	0.573	1.746	0.197
H-Clinoptilolite	$H_6Al_6Si_{30}O_{72}$	2.78	2100	0.355	0.583	1.714	0.207
H-Y	$H_{56}Al_{56}Si_{136}O_{384}$	0.521	15100	0.522	0.787	1.272	0.410
H-Y	ß-cage blocked						0.348

¥ Notes: UC (10^{20}) is the number of unit cells per g of dehydrated zeolite.
UC_V (Å^3) is the Unit Cell Volume.
V_f is the Void Fraction (cc/cc).
ρ (cc/g) is the density of the dehydrated framework.
V_p (cc/g) is the framework Pore Volume per g (dehydrated).

must be equal to the ratio of their liquid densities. Departure from the density ratio for differently sized absorbed molecules indicates that steric constraints are imposed. To provide a measure of the constraint imposed by a framework upon different guest molecules, the concept of 'packing ratio' is introduced. 'Packing ratio' is defined as the ratio of the equilibrium amounts absorbed of two solvents in a given molecular sieve sample; if the solvents are liquid-like in behavior within the framework, then the packing ratio should be identical to the density ratio. If, however, one molecule is more constrained within the framework than another, then the packing ratio will be less than the density ratio. The use of a ratio eliminates the need for an absolute measure of crystallinity for a given sample but serves to describe the packing of solvent molecules in the accessible framework.

For the ZSM-5 study, probe molecules were selected from the alkanes and aromatics to provide information concerning the internal framework volume accessible for absorption, cross-sectional dimensions, and migration limiting features. The interaction of these molecules with molecular sieves (at room temperature) is typical of physical adsorption processes with heats of sorption < 15 kcal/mole. Furthermore, the dimensions of these hydrocarbon molecules are sufficiently different such that slight changes in framework dimensions have profound effects on absorption data.

For the small-pore molecular sieve study, the choice of probe molecules was rather limited; methanol, ethanol, n-propanol, and linear alkanes were generally used. Branched alkanes could not enter such frameworks. For the present study, a compilation of probe molecules and their approximate dimensions is given in Table 2.

3. Characteristic Absorption Values for Zeolite Rho

In preparing a sample for sorption studies, the initial weight loss upon evacuation at 425° C is recorded and represents the desorption of water adsorbed on the surface and from within the framework. As such, the volume calculated from this weight loss from a saturated sample may provide an estimate (providing the sample is not hydrophobic) of the limit to the absorption amounts of other, larger solvent molecules. For zeolite rho, the subsequent absorption of water to measure the framework volume was impractical as the rate of sorption was very slow for all samples examined and the amount sorbed, even after prolonged exposures (~500 hours), did not equal the initial weight loss. However, the sorption of methanol is virtually complete within 3 hours. Shown in Table 5 is a compilation for several rho preparations of the initial weight loss upon evacuation at 425° C and the corresponding pore volume calculated from methanol, MeOH, absorption.

For each sample, the calculated pore volume from methanol absorption agrees very well with the accessible framework volume calculated from the initial weight loss (using a density of 0.998 for water). Thus, methanol absorption seems to provide an accurate measure of the accessible framework pore volume of a rho sample. This measure of

Table 5. Water and methanol absorption[#] data for rho samples.

Form	Calc.	% Wt	Water [#]			MeOH[#]	V_p[†]
@	Temp[*]	Loss[#]	3 h	66 h	100 h	20 h	cc/g
Ca,H	425/Vac	15.0	0.10	5.90		9.71	0.123
La,H	425/Vac	12.6	0.00	2.56		11.07	0.140
H	725/Air	17.4	2.59	12.14	12.49	14.12	0.178
H	600/Ar	24.3	7.25	18.99	18.62	19.53	0.247
H	600/Air	25.0	15.10	19.48	19.71	20.17	0.255
H	550/Air	26.9	15.83	18.62	19.47	21.11	0.267
Li,H	425/Vac	29.1	0.98	7.48		22.42	0.283
H	550/Air	31.4	4.47	21.99	22.02	24.58	0.310
H	500/Air	30.0	11.61	23.81	23.86	24.72	0.312

[#] Dry sample weight basis, sample activated at 425° C and evacuated to $<2x10^{-5}$ torr. Measurements were performed at 27° C and reported as grams absorbed per 100 grams bone-dry sample.

@ Charge compensating cations.

* Calcination conditions, temperature (° C)/ atmosphere.

† Pore Volume, V_p, calculated using a density of 0.792 g/cc for methanol.

accessible framework pore volume is the basis for calculating the amount of size and shape selective phase present in a given sample. It will be compared to the calculated framework pore volume of Table 4.

Almost 200 samples of rho zeolite were examined, about 20 separate preparations with different ion-exchanges and calcination conditions. Shown in Table 6a are the mean absorption values for 43 highly crystalline H-rho samples with a residual cesium content of <1/uc. The H-rho samples were generally prepared by exchanging the Na,Cs-form several times with a 10% NH_4NO_3 solution, washing and drying the material, and calcining in dry nitrogen at 550° C. Statistical analysis of the sorption data for different preparations, modifications, calcinations, etc. is needed to fully characterize and understand the effects of framework topography [16]. The sorption value for methanol, 24.00, corresponds to an accessible void volume of 0.303 cc/g which is in good agreement with the value calculated in Table 4. Thus, under the experimental conditions, methanol fills the available rho framework and packs according to its liquid density.

Table 6a. Characteristic absorption[#] values for zeolite rho - 43 samples, < 1Cs/uc.

Solvent	MeOH	EtOH		nPOH		nHex		iPOH
Time, h	20	3	20	3	20	3	20	20
Mean	24.00	21.12	21.70	14.26	20.20	9.00	10.85	0.89
Std.Dev.	0.89	0.96	0.97	3.88	0.88	2.72	1.66	0.39

[#] g absorbed per 100 grams of dry sample.

Table 6b. Ratios of sorption data - 20 samples.

	Packing Ratios			Rate of Filling Ratios			
	EtOH	nPOH	nPOH	MeOH	EtOH	nPOH	nHex
	MeOH	EtOH	MeOH	3/20	3/20	3/20	3/20
Mean	0.923	0.938	0.871	0.986	0.962	0.958	0.861
Std Dev	0.016	0.013	0.015	0.010	0.025	0.028	0.136
Liquid Density Ratio	0.996	1.019	1.015				

Lower values of methanol sorption indicate that the sample is <100% crystalline, a fraction of the framework pore structure is inaccessible, another phase may be present or, a combination of these possibilities. Use of other techniques, in some cases, provides the reason(s) for the lower framework absorption capacity.

Shown in Table 6b are data for 20 zeolite rho samples with the highest packing and rate of filling ratios. The rate of filling ratio for the solvents decreases as the chain length increases showing one manifestation of steric hindrance. For the C_1-C_3 linear alcohols, equilibrium was reached within 20 hours, longer exposures did not show any additional weight gain within experimental error. The packing ratios are 92-94% of their respective liquid density ratios, again showing the effect of steric constraints. As the guest molecules become longer, the packing ratio decreases. The difference in measured vs. calculated values (from liquid densities) of the packing ratios provides a measure of the constraint imposed on the ethanol and n-propanol molecules by the rho framework. These ratios serve to characterize the rho framework and provide a gauge of the crystallinity of a sample. For example, the samples shown in Table 5 had approximately the same packing ratios as shown in Table 6b. Therefore, the crystallinity of each sample could be estimated by dividing the measured methanol absorption value by the pore volume calculated in Table 4.

Once the sorption parameters for a molecular sieve are well-defined, the constraint

Table 7. Molecular constraint of packing in the zeolite rho framework, < 1Cs/uc.

Molecule	Density g/cc	g absorbed 100 g sample	Volume[#] cc/g	Constraint[†] Index	Molecular Dimensions, Å [11]
Methanol	0.792	24.00	0.3030	1.6	3.6x3.9x4.4
Ethanol	0.789	21.70	0.2750	10.7	3.9x4.2x6.0
n-Propanol	0.804	20.20	0.2512	18.4	3.9x4.3x7.5
n-Hexane	0.659	10.85	0.1646	46.5	3.9x4.3x9.7

[#] Calculated assuming packing as a liquid at 27° C.

[†] Constraint Index is defined as $100*(V_p - \text{Volume}^{\#})/V_p$, where $V_p = 0.3078$ cc/g; the measured packing vs. the liquid density.

placed upon guest molecules can be calculated as shown in Table 7. In this case, the measure of constraint is the liquid density. The inability to assume all configurations of the liquid state is manifested by a low packing ratio or a high 'Constraint Index' and the order of constraint for the rho framework is:

n-hexane >> n-propanol > ethanol > methanol ~ H_2O ~ liquid.

The order of constraint follows the decrease in dimensions of the probe molecules.

4. Distortion of the Zeolite Rho Lattice

As illustrated in Figure 5, empty, the rings of H-rho are nearly circular and the lattice parameter, a, of this cubic zeolite is ~15 Å. However, upon ion-exchange, absorption, temperature, or with the absence or presence of other species in the rho framework, the lattice distorts [17]. The distortion of the double 8-ring in effect serves as a way to modify the aperture or pore dimension. A parameter, Δ, one-half the difference in the length of the major and minor axes of the elliptical 8-ring, was defined. The variation in lattice parameter vs. Δ for rho shown in Figure 6 was caused by the presence of different absorbates as well as different counter ions; in essence, the unit cell could be shrunk almost 25% in volume. In the filled state, with absorbed solvents such as methanol, water, or TMA, the structure is in the unstrained state and the double 8-rings are circular with Δ close to, if not, zero. Empty, the ion-exchanged lattice appears strained and the double 8-rings become orthogonal ellipsoids.

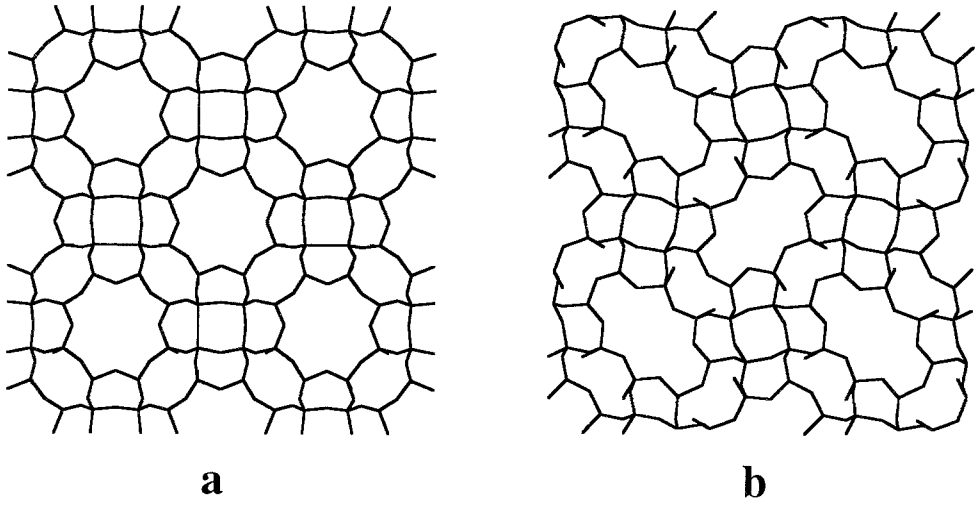

Figure 5. Distortion of the zeolite framework: a) dehydrated H-rho and b) dehydrated Ca,D-rho.

The effect of the size of the charge compensating cations on the sorption properties of zeolite rho can be significant as shown by the data in Table 8. At a nominal loading of six Cs ions per unit cell, absorption into the rho framework is virtually eliminated for methanol and larger probe molecules. Although the Δ is small, Cs sites itself in the double 8-rings and because of its large diameter compared to the nominal 5 Å opening of the rho pores, Cs is able to inhibit the absorption process. Sodium, a somewhat smaller ion, permits methanol to readily enter the framework and provides a fairly sharp size cut-off as shown by the elimination of the absorption of ethanol and larger molecules. For Li and Ca ions, one might expect the sorption process to be faster due to their smaller diameters, but that is not the case and X-ray diffraction provides the rationale. Referring to Figure 6, it is seen that the Δ parameter is quite large for these ions, that is, the double 8-ring is lensed down to a small aperture and produces the observed effect on the sorption process.

Progressive substitution for Cs ions by protons provides the data shown in Table 9. The large diameter of the Cs ion coupled with the relatively small pore diameter of zeolite rho also inhibited the ion-exchange process. Several exchanges with a hot 10% NH_4NO_3 solution were required to reduce the framework Cs content below the 1% level.

Table 8. The effect of charge compensating ions* on the sorption properties of rho.

		g absorbed /100 g sample				Packing Ratios		
Ion*	Diameter	MeOH	MeOH	EtOH	nPOH	EtOH	nPOH	MeOH
	Å	3 h	20 h	20 h	20 h	MeOH	EtOH	3/20
Cs	3.33	1.79	2.12	1.66	0.80	0.783	0.482	0.844
Na	2.04	16.26	18.13	1.80	1.82	0.099	1.011	0.897
Li	1.52	10.92	22.42	20.56	3.80	0.917	0.185	0.487
Ca	2.0	4.84	9.71	1.50	1.40	0.154	0.933	0.498
H		23.66	24.00	21.70	20.20	0.923	0.938	0.986

* at least 6 cations/uc, the remaining charge compensating cations are protons.

Table 9. The effect of cesium on sorption properties of zeolite rho.

	g absorbed / 100g sample				Packing Ratios		Rate of Filling Ratios		
Cs†/uc	MeOH	EtOH	nPOH	nHex	EtOH	nPOH	MeOH	EtOH	nPOH
					MeOH	EtOH	3/20	3/20	3/20
2.67	20.76	13.01	1.00	0.00	0.627	0.077	0.73	0.54	0.42
1.62	21.86	19.61	16.33	0.64	0.897	0.833	0.95	0.91	0.69
0.87	22.96	20.65	17.86	11.14	0.899	0.865	0.95	0.92	0.96
0.50	22.81	20.57	17.84	11.71	0.902	0.867	0.96	0.95	0.97
H	24.00	21.70	20.20	10.85	0.923	0.938	0.99	0.96	0.96

Samples calcined for 4 h at 600° C under dry, flowing nitrogen.

† Cesium ions per unit cell; the remainder of the charge compensating cations are protons.

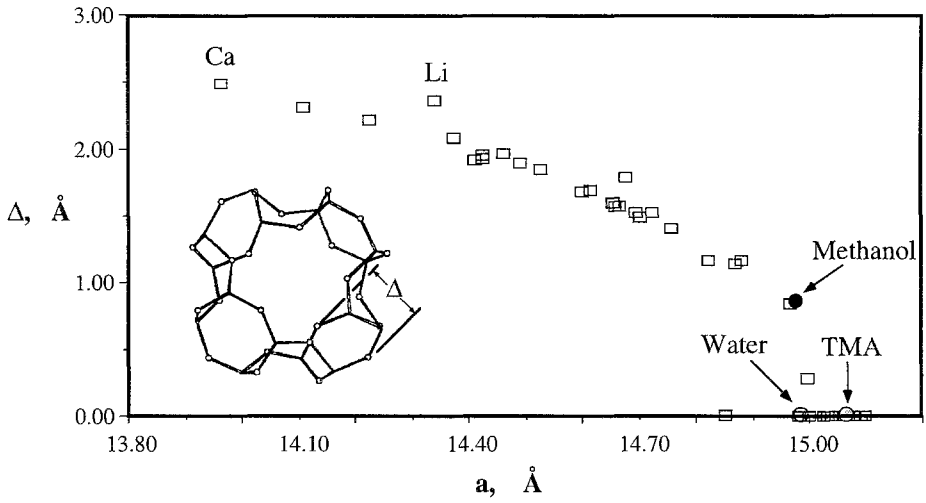

Figure 6. Plot of cell edge (a) vs Δ. The inset illustrates the definition of Δ which is 1/2 the difference in the length of the major and minor axes of the elliptical pore opening.

By carefully manipulating the amount of Cs in the rho framework, the sorption process can be well-controlled and molecules larger than specific sizes can be inhibited from entering the zeolite rho framework; this point is shown graphically in Figure 7.

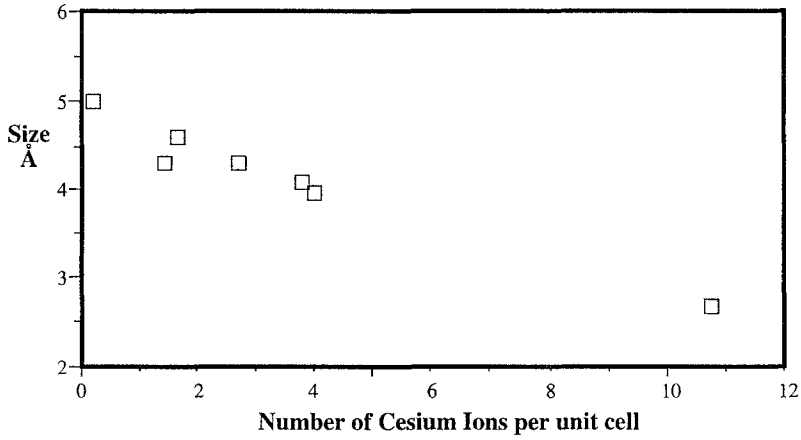

Figure 7. Effect of Cs content on molecular probe exclusion in zeolite rho.

5. Comparison of Rho with Other 8-Ring Zeolites

In our study of the zeolite catalyzed reaction of ammonia with methanol to selectively form dimethylamine, DMA, we found that the selectivity of many zeolite catalysts could be rationalized based on absorption measurements of alcohols at 25° C [16]. For example, low methanol absorption (3-5 wt %) corresponds to low catalytic activity. Compared to trimethylamine, isopropanol is easier to handle while it is very similar in size and shape, and so was used as a gauge to indicate if TMA could readily exit from a zeolite framework. When the framework restricts TMA migration without greatly affecting DMA egress to the product stream, a catalyst may exhibit high DMA selectivity, 60-70%. Isopropanol absorption >3 wt % corresponds to zeolites producing almost a thermodynamic equilibrium distribution of methylamines, TMA ~60-70%. Generally, zeolites, with absorption values for methanol (or ethanol) of 10-30 wt % and little or no isopropanol absorption, selectively produce MMA and DMA versus TMA.

5.1 CHABAZITE

Surprisingly, mineral chabazites provide a wide range of product selectivities towards DMA, although they have almost identical X-ray diffraction patterns and exhibit similar activities. Methanol absorption indicated that the samples' pore volumes were not 100% accessible and suggested the presence of occluded material within the framework. A Geometric Selectivity Index , GSI, was defined as the ratio of methanol absorption to the sorption of n-propanol. Methanol measures the accessible framework capacity while n-propanol sorption (at room temperature) seems to mimic the migration, under reaction conditions, of TMA from the chabazite framework into the product stream. For the variety of chabazite minerals studied, an increase in GSI was found to be directly proportional to an increase in DMA selectivity [16]. This was truly a surprising discovery and underscores the utility of absorption measurements in magnifying small differences in otherwise identical zeolites.

The GSI, however, failed to correctly predict the DMA selectivities for different rho zeolite samples. In this case, we used a microbalance coupled to a mass spectrometer to understand how the different rho samples discharge TMA into the product stream [18]. Mass spectrometry data indicate that, at 200° C, TMA is both physisorbed and chemisorbed with relative amounts of ~10 and ~90%, respectively. For a given zeolite rho sample, the yield of TMA in the methylamines synthesis reaction was found to correlate with the quantity of physisorbed TMA. The physisorbed entity desorbs intactly while the chemisorbed TMA pyrolyzes forming MMA and DMA at normal reaction temperatures.

5.2 ZEOLITE A

The effects of ion-exchange in zeolite A on ethanol packing are summarized in Table 10. By replacing six calcium ions with 12 sodium ions (almost the same size), the internal pore volume is decreased ~5% but the packing of ethanol is affected considerably, ~35% reduction. Exchange with a larger ion, potassium, further reduces the pore volume and virtually prevents ethanol from entering the framework which is indicates that K^+ resides in or near the 8-ring system. Most monovalent ions seem to site in the 8-ring opening so that the pore opening can be controlled somewhat. For the calcium form, no constriction of the pore is observed. The packing and rate of filling ratios are slightly higher for Ca-A than for H-rho especially for n-propanol. Calcium ions site in the 6-ring pores leaving the 8-rings open, and n-propanol easily enters the internal pores of the zeolite. Since the α-cages in the two zeolites are identical, the slight difference in sorption properties is probably caused by the slight constraint imposed by the double 8-ring of rho compared to the single 8-ring in Ca-A.

Table 10a. Effect of ion-exchange on absorption† by zeolite A.

Type	Ion		Calculated Values		Measured Values		
	No./UC	Diameter Å	MeOH	V_p# cc/g	MeOH 20 h	V_p cc/g	% Xtal#
5A	Ca/6	2.00	22.6	0.285	21.7	0.274	96
4A	Na/12	2.04	21.4	0.270	19.4	0.245	91
3A	K/12	2.76	17.2	0.217	16.9	0.213	98

The pore volume and crystallinity values are based on methanol absorption and the inaccessibility of the ß-cages to absorption.

† grams absorbed/100 grams dry sample.

Table 10b. Rate of filling and packing ratios for zeolite A.

Zeolite	Methanol 3/20	Ethanol 3/20	n-Propanol 3/20	EtOH MeOH	nPOH EtOH	nPOH MeOH
5A	0.981	0.95	0.93	0.97	0.94	0.90
4A	0.90	0.4	0.2	0.62		
3A	0.85	0.1		0.24		

5.3 ZK-5

ZK-5 has α-cages like zeolites rho and A but the cages are joined by bridged double 8-rings (see Figure 8). As shown in Table 11, the EtOH:MeOH packing ratio approaches

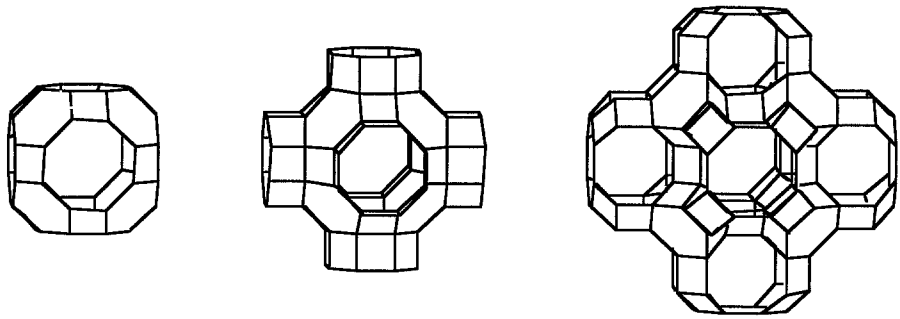

Figure 8. Structures of the α-cages and interconnections between α-cages for zeolites a) A, b) rho, and c) ZK-5.

Table 11. Absorption properties of H-ZK-5.

Measured Values			Packing Ratios		
MeOH†	Vp	%	EtOH	nPOH	nPOH
20 h	cc/g	Xtal	MeOH	EtOH	MeOH
20.4	0.257	84.2	0.955	0.839	0.801
19.8	0.250	81.9	0.975	0.762	0.743
19.5	0.246	80.6	0.977	0.708	0.692
19.9	0.251	82.3	0.953	0.677	0.645
20.0	0.253	83	0.883	0.628	0.554
20.3	0.257	84.2	0.945	0.604	0.571
19.1	0.241	79.1	0.993	0.573	0.569
19.9	0.251	82.2	0.955	0.358	0.342
16.7	0.210	68.9	0.994	0.357	0.355
19.4	0.244	80.1	0.889	0.303	0.269
18.6	0.235	76.9	0.992	0.282	0.280
22.0	0.278	91.2	0.876	0.115	0.101
19.8	0.250	82	0.987	0.108	0.106
19.5	0.246	80.7	0.865	0.046	0.040
17.2	0.217	71.3	0.766	0.010	0.008

† g methanol absorbed per 100 grams dry sample. The crystallinity is calculated on the basis of the methanol pore volume with 100% being equivalent to 0.305 cc/g.

1.0 and clearly demonstrates the effect of small changes in framework geometry on sorbate molecular packing. Another consequence of the structural differences shows up in the retention of framework crystallinity after calcination. Although calcined under almost identical conditions as zeolite rho to convert the ammonium form to the H-form, ZK-5 has lost significant amounts of crystallinity. Most of the resulting silica-alumina species remain within the framework as evidenced by the drastic lowering of the other packing ratios. This observation underscores the need to use molecules of different sizes (and/or shapes) to characterize accessible framework volumes. Reliance solely on the EtOH:MeOH packing ratio would be quite misleading especially if these samples were used for measuring the kinetics of absorption of n-propanol, hexane, etc.

5.4 EFFECT OF Si/Al RATIO

The Si/Al ratios for zeolites rho, ZK-5, A are 3, 2.2, 1, respectively. The packing ratios suggest that zeolite A has less constraint on nPOH than does zeolite rho; the slight increase in packing ratio is probably caused by the slightly larger bond and cage dimensions due to the higher Al content. The increase in pore volume is much less than anticipated by consideration of normal Al-O bond lengths because the bond length in zeolites is closer to the Si-O bond length. No unambiguous conclusion can be made for zeolite ZK-5 because of the extensive damage suffered during the calcination process to convert it to the H^+ form. Small occlusions within the framework can drastically affect packing ratios as shown in Table 11. For zeolite ZK-5, although most samples had greater than 80% crystallinity, there is a large variation in the nPOH:EtOH and nPOH:MeOH packing ratios. Appropriate calcination conditions were not found which would convert the ammonium form to the proton form while retaining all of the framework crystallinity. The instability of some frameworks in the proton form is not surprising. Zeolite ammonium-A will completely decompose if heated around 300°C.

5.5 CALCINATION OF MOLECULAR SIEVES

Calcination of molecular sieves was used to provide some understanding of their thermal stability as well as to provide samples with controlled changes in amounts of crystallinity and to determine what the effects on sorption properties would be. Such knowledge is important because:

- NH_4^+ containing zeolites are calcined to provide the acid H^+ form.
- molecular sieves are heated in some uses as well as during regeneration cycles to drive off absorbed species.
- if decomposition of the framework occurs, what is the fate of the decomposed material and what does it do with respect to the sieve's absorption properties?

Some of the effects of calcining a sample of zeolite rho are listed in Table 12. For comparison purposes, the expectation values for a typical sample of rho zeolite are

included. The increase in sorption values upon calcining at 600° C rather than 500° C is attributed to the removal of small amounts of ammonium ion that had not dissociated during the 500° C calcination process. IR spectroscopy confirmed the presence of NH_4^+ in the lower calcination temperature sample. The small residual amount had a large effect on the amount of n-propanol absorbed as well as its 'rate of filling' ratio. At 600°C, ammonium ion was no longer detected. The crystallinity of the 600° C sample is around 88% (21.13/24) and one is prompted to ask 'what effect does the 12% lack of crystallinity have on the sorption properties?'. Since the packing ratios are the same as found for a typical rho zeolite, this suggests that the non-absorbing material either blocks off a portion of the framework or resides on the exterior surface of the crystals. If it were to reside within an accessible part of the framework, the packing ratios would be lower. The fact that the rate of filling ratio for n-propanol is much lower than that of a typical sample suggests that the non-absorbing material is on the external surface of the crystals near the pore openings such that it slows down the sorption process.

Upon raising the calcination temperature to 700° C and using undried nitrogen (probably 5-10 torr of water vapor was present), the changes produced by calcination are much more dramatic. In this case, 'house' nitrogen (the supply to our entire building) was used rather than a special tank of dry, high purity grade used to obtain BET surface areas. The sample's crystallinity has dropped to 51% and the propanol and hexane sorption was almost eliminated. The reduction in packing ratios reflects sizeable migration of the decomposed material within the framework. By contrast, calcination of other zeolite rho preparations in a very dry environment does not produce equivalent or larger effects even at 800° C as shown in Table 13. The calcining of zeolite rho and the effects produced vary somewhat depending upon the preparation. The amount of framework decomposed certainly increases as the calcination temperature increases but the trends in packing ratio vary erratically while the rate of filling ratios clearly decrease. For the most part, calcination under dry conditions does not provide a mechanism for material migration; the decomposed framework seems to remain in place. By contrast, as shown in Table 12, small amounts of water vapor facilitate the decomposition and migration processes.

Table 12. Effect of calcination on the sorption values of a H-rho zeolite sample.

	g absorbed/100g sample				Packing Ratios		Rate of Filling	
Calc. Temp., °C	MeOH	EtOH	nPOH	nHex	EtOH / MeOH	nPOH / EtOH	EtOH 3/20	nPOH 3/20
Typical	24.00	21.70	20.20	10.85	0.923	0.938	0.96	0.96
500†	20.20	18.18	12.27	4.77	0.900	0.675	0.97	0.58
600†	21.13	19.51	17.95	9.58	0.923	0.920	0.88	0.71
700*	12.66	9.16	1.99	0.37	0.723	0.218	0.81	0.44

† Calcined in a shallow bed for 4 hours under dry, flowing nitrogen.

* Calcined under flowing nitrogen (not dried) for 4 h.

Table 13. Calcination of different preparations of zeolite rho..

	Calc.				Packing Ratios		Rate of Filling Ratios	
	Temp	g absorbed/100 g sample			EtOH	nPOH	EtOH	nPOH
Prep	° C†	MeOH	EtOH	nPOH	MeOH	EtOH	3/20	3/20
1	600	19.37	18.35	15.67	0.947	0.854	0.89	0.54
1	700	18.62	17.71	15.36	0.951	0.867	0.88	0.31
2	600	22.23	20.93	18.71	0.942	0.894	0.99	0.98
2	700	19.77	18.01	16.93	0.911	0.940	0.96	0.95
2	800	17.64	15.76	15.25	0.894	0.968	0.95	0.94
3	600	20.85	19.95	17.10	0.957	0.857	0.96	0.97
3	800	19.11	17.35	15.32	0.908	0.883	0.94	0.94
Typical		24.00	21.70	20.20	0.923	0.938	0.96	0.96

† Samples were calcined under dry flowing nitrogen for 4 h at the temperatures noted.

6. Characterization of ZSM-5 by Sorption Measurements

The pentasil family of zeolites, which includes ZSM-5, has exhibited very valuable catalytic properties including high chemical selectivity, low coking (aging) tendency, and high turnover activity for a variety of chemical reactions [19]. The impressive catalytic selectivity and in-use stability of the pentasil family of zeolites are attributed to a unique combination of properties, such as size, shape, and site sorption selectivities, chemistry, and substrate diffusion on the internal surface. X-Ray diffraction analyses show that ZSM-5 possesses two types of pores, both of which are composed of 10 tetrahedral-membered rings: one pore system is sinusoidal with a nearly circular cross section, while the other is straight and perpendicular to the sinusoidal system with elliptical pores. A representation of the internal surface of the channels (void space) of the ZSM-5 internal framework is shown schematically in Figure 9.

For the sorption of n-hexane into the H-ZSM-5 framework, there is a range of values 10-14 g/100 g reported in the literature [19,20]. There are several causes for the variety of values for the amount of n-hexane sorbed. As noted above, the duration of exposure is very important because of the slow absorption rates that are common during the final stages of filling the framework. Too short exposures to solvent vapors yield low 'equilibrium' absorption values. Furthermore, as noted earlier, a rigorous vacuum heat treatment is needed to prepare a molecular sieve for sorption studies. If some residue were contained in the framework, absorption values would tend to be lower. Another reason for low absorption values is a poorly crystalline sample or a sample with a non-zeolitic component. For high surface area solids, the external surface can make a

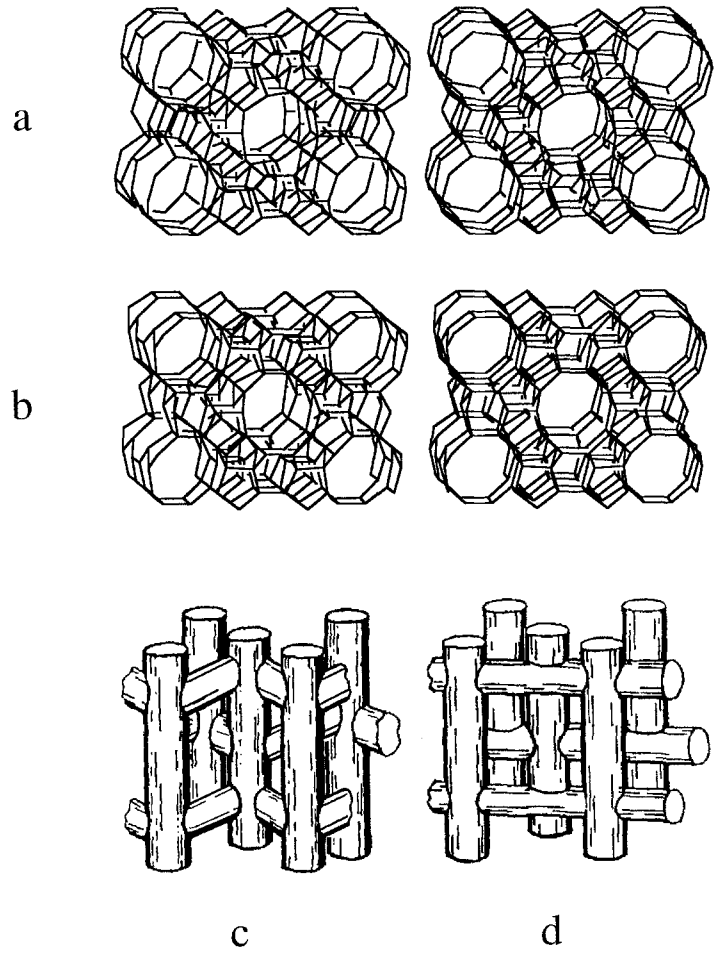

Figure 9. Stereographic drawings of the frameworks of a) ZSM-5 and b) ZSM-11 as well as representations of the void space (channel) structures of c) ZSM-5 and d) ZSM-11.

significant contribution to the sorption isotherm, generally in the range 5 to 20% of the total amount. Adsorption, if unaccounted for, would provide higher than expected absorption values. Interestingly, most investigators neglect surface contributions.

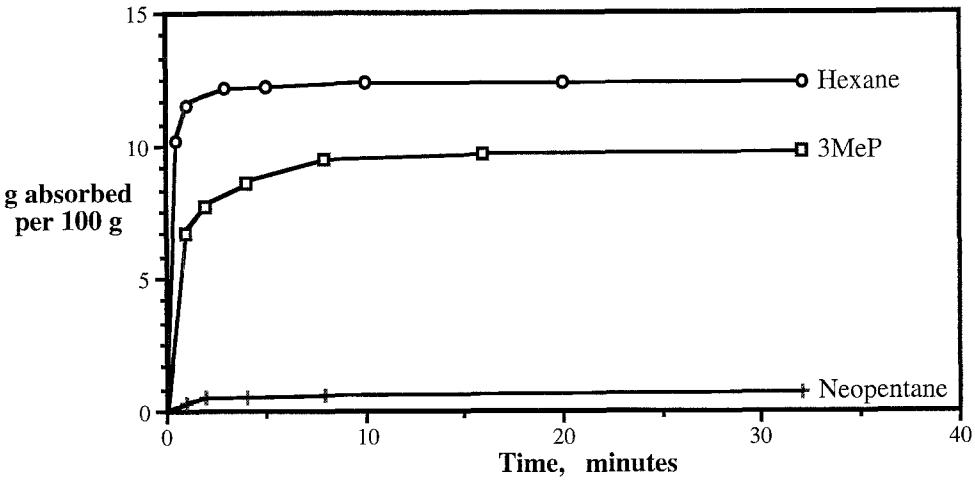

Figure 10. Absorption data for hexane, 3-methylpentane (3MeP), and neopentane into a sample of H-ZSM-5.

Shown in Figure 10 are the data for the absorption of three alkanes into a sample of H-ZSM-5. Hexane absorbs quickly into this sample of H-ZSM-5 and reaches about 95% of the final absorbed amount (0.125 g/g at 20 hours for this sample) in five minutes. The absorption of 3-methylpentane, 3MeP, a branched isomer of hexane, is somewhat slower as shown by the rounded 'knee' at a longer time in the sorption-time plot. The sorption of 2,2-dimethylpropane, neopentane, is very slow and continues for weeks without equilibrating. The relative diffusion rates of these sorbates can be estimated from the data [21] and decrease with an increase in cross-sectional dimensions of the molecules:

hexane:3MeP:neopentane = 0.92:0.25:0.001 = 3.9x4.3:5.1x5.9:5.5x5.8 Å

If a value of 6.8 Å is chosen as the 'critical' (smallest) pore dimension of ZSM-5 common to all the data, then the relative absorption rate-size data above correspond reasonably well to the correlation of Moore and Katzer [14]. The value for the pore dimension is close to the value in Table 1 estimated for covalent oxygen in a 10-membered ring.

As noted, the absorption of hexane into H-ZSM-5 is fairly rapid and reaches an apparent 'end point' or equilibrium value; the 3 and 20 hour sorption readings are the same within experimental error. A mean value of 13.07 g/100 g (std dev 0.27) was determined (for 29 highly crystalline samples prepared using tetrapropylammonium ion, TPA, as the templating ion) which corresponds to a framework volume of 0.198 (std dev 0.004) cc/g using a value of 0.659 g/cc as the density for hexane. Thus, hexane appears to fill the H-ZSM-5 framework in a 'liquid-like' manner as the volume of hexane absorbed agrees well, within experimental error, with the calculated framework volume

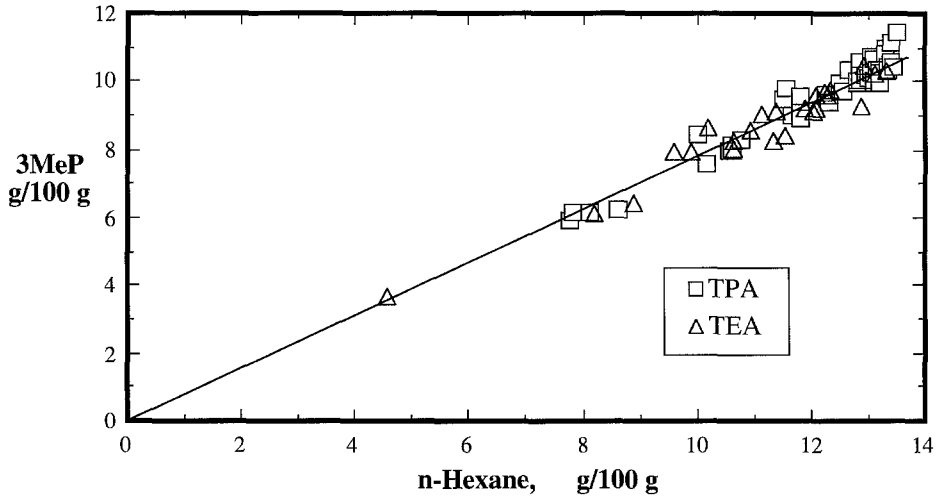

Figure 11. Absorption data for 3-methylpentane (3MeP) vs. n-hexane into samples of ZSM-5 prepared using TPA and TEA templates.

capacity (Table 4). Samples of H-ZSM-5 had Si/Al ratios ranging from 11 to >1000; the amount of aluminum in the framework did not appear to affect the value of hexane absorbed.

As shown in Figure 10, 3MeP is also absorbed rapidly into the H-ZSM-5 framework. Its liquid density is sufficiently close to that of hexane such that, if steric constraints were not imposed by the framework on the packing of 3MeP, the same sorption weight gain would be obtained. But, H-ZSM-5 samples absorb a significantly smaller amount of 3MeP compared to hexane. Shown in Figure 11 is the sorption data for 3MeP and hexane for a variety of H-ZSM-5 samples (included in this figure are data using two different synthesis template molecules; this will be discussed further). For a given sample, the amount of 3MeP absorbed is plotted versus its hexane absorption value. From the Figure, it is seen that the absorption ratio 3MeP:hexane is independent of the amount of hexane absorbed (that is, it is independent of the crystallinity of the sample). The packing ratio, 3MeP/Hex, of 0.789 (std. dev. 0.023 for 39 samples) is characteristic of the H-ZSM-5 framework. Similarly, the absorption of *p*-xylene is directly related to the hexane absorption amount with a packing ratio of 1.218 (std. dev. 0.045 for 30 samples); this is shown graphically as Figure 12. Again, the amount of aluminum in the framework did not seem to affect the observed ratio. Samples of H-ZSM-5 displaying these characteristic ratios have their crystallinity determined by dividing the hexane sorption by 13.07.

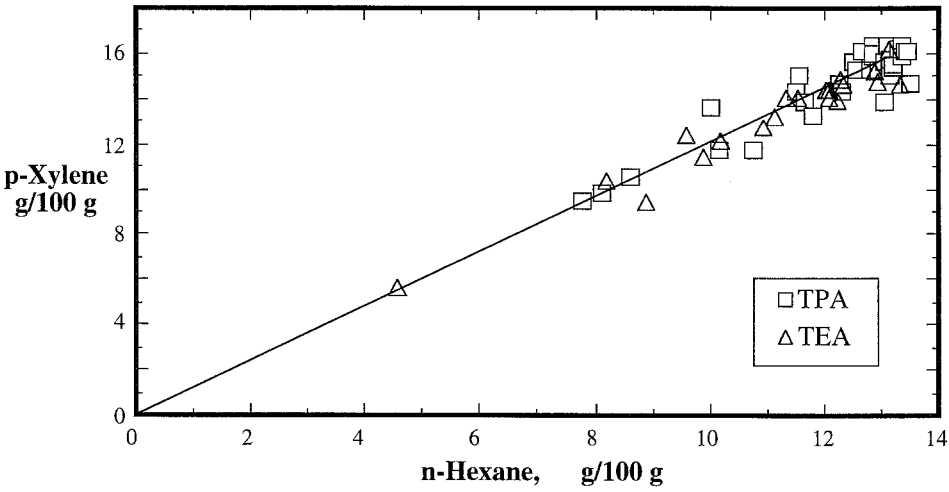

Figure 12. Absorption data for *p*-xylene vs. n-hexane into samples of ZSM-5 prepared using TPA and TEA templates.

Table 14. Characteristic absorption values for H-ZSM-5 (TPA template, 58 samples).

Solvent	g absorbed/ 100 g sample	Std Dev	No. #	Packing Ratio†	Density Ratio∂	Constraint Index®	Molecular Dimensions, Å [11]
n-Hexane	13.07	0.03	29	1.000	1.00	0	3.9x4.3x9.7
p-Xylene	15.78	0.43	22	1.218	1.31	7.5	3.6x6.5x8.9
3-Methylpentane	10.36	0.32	27	0.789	1.01	22.4	5.1x5.9x8.0
Toluene	12.91	1.03	14	0.974	1.31	25.5	3.6x6.5x8.1
Benzene	11.29	0.53	20	0.888	1.33	35.8	2.5x6.5x7.2
Carbon Tetrachloride	15.23	0.64	20	1.177	2.42	52.2	5.4
Cyclohexane	7.38	0.98	29	0.638	1.18	52.6	5.1x6.0x6.5

The number of values used to obtained the reported data.

† The ratio of the amount absorbed to the amount of hexane absorbed.

∂ The ratio of the solvent density to the density of hexane.

® The (density ratio minus the packing ratio) divided by the density ratio x 100.

Shown in Table 14 are the equilibrium sorption data, at 20 hours, for a variety of solvents and the packing ratios are characteristic values for H-ZSM-5. Hexane and smaller molecules (for example, butane, pentane, CO_2) pack according to their liquid densities; the same framework volume is accessible to all of these molecules. The other, larger, molecules listed in Table 14 are all constrained in some fashion.

Interestingly, the packing ratios for *p*-xylene:benzene and toluene:benzene are 1.384 (std. dev. 0.046 for 25 samples) and 1.122 (std. dev. 0.097 for 24 samples), respectively. Within experimental error, these ratios are almost equal to the ratios of their molecular weights which suggests that the molecules pack with the same number per unit cell. The relative lengths of these molecules are, however, in the ratio 1:24:1.12:1 (pxyl:tol:bz) such that packing by length cannot solely account for the measured absorption data.

For larger molecules, such as *o*- and *m*-xylenes, 2,2-dimethylbutane, and neopentane, the sorptions are not equilibrated at 20 hours; extending the measurements to one week still did not provide equilibrium data. For a given sample, *o*-xylene (3.6x7.1 Å) sorbs almost twice as fast into the H-ZSM-5 framework as does *m*-xylene (3.6x7.2 Å). Again, using the correlation of Moore and Katzer, the sorption rates correspond to the difference in the xylenes' cross-sectional dimensions; for diffusion into the same framework, a difference of 0.1 Å in molecular dimension corresponds to a factor of two in rate. The absorption rate of the large molecules into various H-ZSM-5 samples varies from sample to sample and suggests that their pore openings (and/or external surface area) are different. The different rates of sorption of *o*-xylene into ZSM-5 samples can be used to distinguish the various samples from each other even though they have similar hexane sorptions (similar crystallinities); *o*-xylene absorption values at 20 hours ranging from 0.37 to 9.7 g/100 G were obtained for 55 samples. Assuming that Moore and Katzer's correlation is correct, the overall variation in diffusion coefficients corresponds to a difference of 0.6 Å in pore dimension because the molecular probe, *o*-xylene, was kept constant. This difference in size is close to the size difference in pores for the straight and sinusoidal channels of the ZSM-5 framework. Values in between the extremes suggest a mix of the two channel systems.

6.1 COMPARISON OF TPA AND TEA PREPARATIONS OF ZSM-5

ZSM-5 can be prepared using a variety of template molecules; the data in Table 14 were obtained for samples prepared using tetrapropylammonium ion, TPA, as the template. For comparison, tetraethylammonium ion, TEA, was used as the template. The crystals have morphology (stubby, elliptical cylinders with flat ends) that is significantly different from the usual ZSM-5 crystal configuration of right-angle, prismatic, penetration twins obtained when TPA is used as the templating ion. However, the X-ray diffraction patterns of the TEA preparations are virtually indistinguishable from those using TPA. As shown in Figure 11, the absorption data for 3MeP vs. n-hexane does not distinguish the preparations on the basis of the template ion that was used. Further, as shown in Figure 12, absorption of a slightly larger molecule, *p*-xylene, doesn't clearly distinguish

the different templated preparations. The error in the absorption measurements is larger than any difference in the framework structures. Table 15 summarizes the absorption data for the TEA templated preparations.

Table 15. Characteristic absorption values for H-ZSM-5 (TEA template, 24 samples).

Solvent	g absorbed/ 100 g sample	Std Dev	No. #	Packing Ratio†	Density Ratio∂	Constraint Index®
n-Hexane	12.56	0.49	10	1.000	1.00	0
p-Xylene	14.54	0.64	11	1.191	1.31	9
3-Methylpentane	9.68	0.47	10	0.777	1.01	23
Toluene	9.09	1.17	8	0.74	1.31	44
Benzene	8.09	0.73	13	0.66	1.33	50
Carbon Tetrachloride	11.58	1.07	9	0.94	2.42	61
Cyclohexane	4.43	1.30	13	0.34	1.18	71

The number of values used to obtained the reported data.

† The ratio of the amount absorbed to the amount of hexane absorbed.

∂ The ratio of the solvent density to the density of hexane.

® The (density ratio minus the packing ratio) divided by the density ratio x 100.

For molecules the size of hexane and smaller, the absorption data, within experimental error, is the same for the TPA and TEA template preparations. As with the X-ray diffraction patterns for the two different templated materials, the packing ratios of *p*-xylene:hexane and 3MeP:hexane also suggest that the zeolites are very similar, if not identical. However, as the size of the probe molecule increases, the constraint presented by the TEA framework is larger than the constraint exerted by TPA system. This observation suggests that the TEA preparations have slightly smaller channel dimensions than the TPA preparations and this difference is magnified as the absorbing molecule gets larger.

As noted above, ZSM-5 crystals have two slightly different channel systems capable of absorbing molecules. For the TPA template, conditions during the synthesis of a sample cause one channel system to dominate over the other, thereby providing a spectrum of sorption rates for large molecules. Using TEA as the template molecule seems to alter the crystal morphology and let the smaller channels dominate. The difference in channel dimension and relative channel population imposes greater constraint on the packing of probe molecules as they increase in size; this is consistent with the data shown in Tables 14 and 15. Thus, the choice of template molecule seems to control the external morphology of the ZSM-5 crystals, which channel system dominates, and the rates of absorption and amount absorbed into the framework.

6.2 CHARACTERIZATION OF ZSM-11 BY SORPTION MEASUREMENTS

The zeolite ZSM-11 also belongs to the pentasil family; it has two channels which, unlike ZSM-5, are straight and nearly circular (see Figure 9). Although we didn't prepare and characterize as many ZSM-11 samples as we did for ZSM-5, the few absorption values seem to confirm that ZSM-11 channels are slightly larger and constrain the probe molecules somewhat less than ZSM-5 as shown in Table 16. The rates of absorption of *o*- and *m*-xylenes into the framework seem to be higher for ZSM-11 than for ZSM-5 but the statistics may be faulty as there were not that many samples prepared and tested. Further, as noted for ZSM-5, the absorption of large molecules such as *o*- and *m*-xylenes did not equilibrate even after one week of exposure.

Table 16. Characteristic absorption values for H-ZSM-11 (9 samples).

Solvent	g absorbed/ 100 g sample	Std Dev	No. #	Packing Ratio†	Density Ratio∂	Constraint Index®	ZSM-5 Constraint
n-Hexane	13.52	0.33	5	1.000	1.00	0	0
3-Methylpentane	10.79	0.24	5	0.797	1.01	21	22
Carbon Tetrachloride	15.55		2	1.150	2.42	52	52
Cyclohexane	8.42	0.51	9	0.623	1.18	47	53

The number of values used to obtained the reported data.

† The ratio of the amount absorbed to the amount of hexane absorbed.

∂ The ratio of the solvent density to the density of hexane.

® The (density ratio minus the packing ratio) divided by the density ratio x 100.

7. Quantitative Aspects of Adsorption Measurements

Although there are numerous papers reporting on the characterization of zeolites, few deal with the problem of quantifying the amount of molecular sieve present in a sample. Gabelica et al. used X-ray diffraction, DTA, and NMR to characterize ZSM-5 preparations [22]. Derouane et al. used thermogravimetric analysis to follow the decomposition of the organic template ion in ZSM-5 preparations and calculated crystallinities from that data [23]. Jacobs et al. used IR spectroscopy to quantify the presence of crystalline ZSM-5 in X-ray amorphous samples [24]. Whether examining laboratory synthesized preparations as these investigators have done or examining natural minerals, it is desirable to know how much of the material present is zeolitic vis-a-vis, for example, an amorphous aluminosilicate. The use of absorption can provide a means to quantify the amount of molecular sieve in a given sample. For a given framework, by using the absorption of appropriately sized probe molecules, a set of packing ratios and specific absorption amounts can be determined. For any sample of that framework, X-ray diffraction is used to make sure that there is no other framework species present to any

large extent. Then, the samples' absorption values are used to quantify the amount of molecular sieve phase present (crystallinity) or accessible.

7.1 COMPARISON OF CRYSTALLINITY MEASUREMENTS: X-RAY DIFFRACTION VS. ABSORPTION

It is common practice to use the intensity of some X-ray diffraction peaks as the basis for declaring molecular sieves to be 100% crystalline especially in the absence of other phases. However, X-ray diffraction is not a sufficiently sensitive tool for this task because the unit cells of many molecular sieves are on the order of 15-20 Å in size while large crystals, that is, much longer range ordering, are needed to clearly describe the resulting frameworks in XRD. In the synthesis process, small groupings (2-3 unit cells wide) can form and they may not be visible to X-ray diffraction - in fact, such preparations have been named 'X-ray amorphous'.

Shown in Figure 13 are the X-ray patterns of a highly crystalline ZSM-5 sample and one that appears to be ~25% crystalline; it has an average crystallite size of 300 Å estimated from line broadening (Debye-Scherer). Absorption of hexane, 3MeP, and *p*-xylene show typical ZSM-5 packing ratios from which it was determined that the sample is about 60% crystalline. The apparent discrepancy in crystallinity was resolved by using high resolution electron microscopy which revealed small domains of 60-80 Å within many particles of the preparation. These small domains account for the X-ray line broadening, the poor quality of the X-ray diffraction pattern, and the fact that crystallinity via absorption was significantly higher than via X-ray diffraction. What is so fascinating is that the domains, although small and disoriented, are almost completely accessible for absorption and that they show typical ZSM-5 packing fractions.

During the synthesis of molecular sieves, it is essential to know when the appropriate moment arrives to stop the synthesis and recover the product. If the synthesis were allowed to proceed unchecked, many zeolites would transform to other unwanted phases. This is the so-called 'art' of molecular sieve synthesis. However, by carefully controlling synthesis procedures and characterizing the products at various times during the synthesis, some of the 'art' can be eliminated. Shown in Table 17 is a comparison of the X-ray diffraction data, surface area measurements, and sorption data for samples of rho zeolite extracted from the synthesis autoclave. Following normal work-up procedures, the samples were ion-exchanged with NH_4NO_3 and calcined at 550° C to convert them to the H^+ form. As the synthesis proceeds, the X-ray counts remain quite low, the surface area decreases rapidly and, prior to collecting the 48 hour sample, the sorption values for the alcohols are almost identical, independent of molecular size. By not correcting for surface adsorption, the sorption values, shown in Table 17, can be quite misleading. The packing ratios are close to the density ratios, especially the iPOH:MeOH value, which is typical of surface adsorption. At 48 hours in the synthesis, the iPOH:MeOH packing ratio drops significantly towards the value 0.04, the value typical of a highly crystalline rho sample.

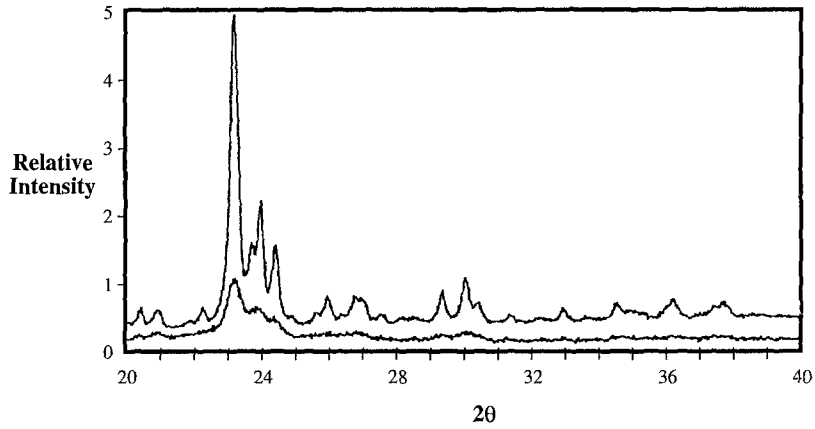

Figure 13. X-Ray powder diffraction patterns for a highly crystalline sample of ZSM-5 and one that is approximately 25% crystalline by XRD.

Correction of the sorption data for adsorption effects in the 32 h and earlier samples reveals that there is no framework absorption. Shown as Table 18 are the data for the 48 h and later samples corrected for adsorption. Both the 56 and 72 h samples are highly crystalline via X-ray diffraction. But absorption shows that something occurred during the synthesis, exchange, or calcination because, for the 72 h sample, the rate of

Table 17. The synthesis of zeolite rho: the first 48 hours.

							Packing Ratios		
Prep#	APD$	SA†	g sorbed®/ 100 g dry sample				EtOH	nPOH	iPOH
Time	cps	m^2/g	MeOH	EtOH	nPOH	iPOH	MeOH	MeOH	MeOH
0	41	218	3.75	4.52	5.16	4.86	1.205	1.376	1.296
8	225	208	4.56	4.31	4.80	4.60	0.945	1.053	1.009
24	53	131	2.83	2.69	3.06	2.96	0.951	1.081	1.046
32	32	112	2.55	2.25	2.60	2.52	0.882	1.020	0.988
48	346	87	6.76	5.58	5.50	1.97	0.825	0.814	0.291

Hours in synthesis reactor, temperature 100° C.

$ Automatic Powder Diffraction camera, counts per second of major X-ray diffraction peak; the expectation for a highly crystalline sample is 1700-1800 cps.

† Surface areas, ±2 m^2/g, determined by adsorption and mercury porosimetry; 30-40 m^2/g is typical of a highly crystalline sample.

® Total sorbed amounts: no correction for adsorption on external surfaces.

Table 18. Corrected absorption data for zeolite rho sampled during synthesis.

					Packing Ratios		Rate of Filling Ratios		
Prep.	g absorbed/100 g sample			Xtal†	EtOH	nPOH	MeOH	EtOH	nPOH
Time	MeOH	EtOH	nPOH	%	MeOH	EtOH	3/20	3/20	3/20
48	4.86	4.69	3.38	20.2	0.964	0.721	0.92	0.89	0.53
56	17.50	16.30	13.94	72.9	0.931	0.855	0.96	0.96	0.51
72	23.22	21.60	5.93	96.7	0.930	0.275	0.34	0.14	0.04
Typical	24.00	21.70	20.20	100	0.923	0.938	0.99	0.96	0.96

† per cent crystallinity - basis: 24 g/100 g of methanol is equivalent to 100% crystallinity.

adsorption of the linear alcohols and nPOH:EtOH packing ratio are much lower than usual. The presence of a sharp X-ray diffraction pattern is no guarantee for the synthesis of a well-behaved molecular sieve. This example clearly demonstrates the fact that absorption and X-ray diffraction measurements are complementary techniques and both are needed in characterization of molecular sieves.

8. Catalysis and Reactions Using Molecular Sieves as Supports

As noted above, molecular sieves are used as absorbents where a probe molecule's size and shape play important roles in the sorption process. The situation is similar when sieves are used as catalysts or supports for a reaction. As such, reactions and their product distributions can be used to characterize the framework topology, connectivity, and dimensions of molecular sieves. At least three types of reaction selectivity over zeolite catalysts have been described [25].

- Product selectivity. Molecular sieving selectivity of the zeolite provides the basis for determining the product spectrum: molecules smaller than the pore openings can exit from the framework into the product stream while larger molecules are retained within the framework.
- Transition state selectivity. Certain reactions are prevented because the corresponding transition state requires more space than is available within the framework of the zeolites.
- Reactant selectivity. Only those components of the feed stream that are small enough to enter the pores can react while larger ones are excluded.

As a practical application, zeolite H-ZSM-5 has been used as a catalyst for the conversion of pseudocumene and methanol to durene [26]. Different preparations of ZSM-5 gave different durene yields without any rational basis. Consider that the cross-section of durene is almost identical to *o*-xylene; sorption of *o*-xylene was shown to correlate with the catalytic selectivity towards durene. Thus, very slight differences in the accessible channel dimensions may have a profound affect on the catalytic selectivity.

8.1 USE OF ABSORPTION IN CATALYST DESIGN AND MODIFICATION

In the production of ethylene from the cracking of natural gas, small amounts of acetylene and butadiene are produced. Acetylene can present a hazard while non-selective hydrogenation removes valuable ethylene and butadiene as well as the target acetylene. A process improvement would eliminate acetylene from the product stream yet permit full recovery of butadiene and ethylene. The catalysts generally used are active metals supported on "inert" substrates but both acetylene and butadiene are hydrogenated to a substantial degree. Therefore, in the design of a new catalyst, these considerations were taken into account:

- selective hydrogenation of acetylene versus butadiene and ethylene.
- hydrogenation of acetylene to ethylene is preferable.
- minimal hydrogenation of butadiene and ethylene.
- the economics of plant investment.

Placing the active metal catalyst inside a small pore zeolite takes advantage of the differences in size and shape of the acetylene, butadiene, and ethylene molecules and establishes kinetic control over the hydrogenation [27]. Butadiene, because of its larger size, would be excluded from entering the zeolite framework which is accessible to the smaller acetylene and ethylene molecules. Then, acetylene could be hydrogenated within the framework at active metal sites within the pores while butadiene, because it cannot enter the framework, passes through the bed unreacted. Zeolite A was selected as the catalyst support because of its appropriate pore dimension, availability, cost, and the ability to be ion-exchanged which would control the transport processes. Absorption measurements could then be used to design and fine-tune the catalysts which were ion-exchanged with a small amount of Ni^{2+} and subsequently reduced.

The linear C_1-C_3 alcohols were used as probes for the study. If methanol could freely enter the zeolite, so could the smaller acetylene. Ethanol and propanol bracket butadiene in size. If propanol would have free access to the framework, so would butadiene. If the access of ethanol were restricted, then butadiene would be prevented from entering the framework (and hydrogenating). From the data presented in Table 19, it is apparent that the degree of ion-exchange and the size of the charge compensating cation, M, have profound influences on the amounts absorbed by the framework.

Reduction in methanol sorption capacity indicates decreased internal pore volume and relates to the exchanged ionic size and the amount of charge compensating cation. The Ca sample shows little differentiation for any alcohol which indicates that this sample should not be a selective catalyst (it wasn't). Calcium ions site in the 6-ring pores leaving the 8-rings open, and n-propanol easily enters the internal pores of the zeolite. Because it is smaller in size than n-propanol, butadiene should also access the internal framework of this sample. As in this case, if the active catalytic sites are within the framework and butadiene can access them, butadiene will also be hydrogenated.

Table 19. Absorption results for Zeolite Ni,M-A (Ni^0 is the active catalyst).

Ions#	Absorption Data			Packing Ratios			Volumes, cc/g		Occ
M	MeOH	EtOH	nPOH	EtOH / MeOH	nPOH / EtOH	nPOH / MeOH	Acc @	MeOH &	% †
Ca	21.9	19.9	18.6	0.908	0.935	0.85	0.278	0.28	99.3
Na	19.5	16.3	9.6	0.836	0.586	0.49	0.281	0.25	87.5
K-1®	17	11.4	0.45	0.666	0.04	0.03	0.246	0.22	87.2
K-2®	16.5	1.7	0	0.106	0	0	0.236	0.21	88.1
Rb	14.6	8.6	0	0.589	0	0	0.224	0.18	82.2
Cs	10.6	0.19	0	0.018	0	0	0.202	0.13	66.4

\# M, the major cation: Ca^{+2}, K^+, Na^+, Rb^+, Cs^+.

@ the accessible framework volume taking into account the ionic volumes.

& the framework volume occupied by methanol assuming packing as a liquid.

† the percent occupancy of the accessible framework.

® K-2 has a higher percent of K^+ as charge compensating ion than K-1.

The Na sample exhibits some pore narrowing (as evidenced by reduced n-propanol sorption) which should translate to reduced sorption of the butadiene molecule. In the cases of the K^+, Rb^+, and Cs^+ exchanged forms, essentially no n-propanol is absorbed and ethanol sorption is significantly lowered for some samples; these catalysts should show a reduction in the hydrogenation of butadiene. Here, fine-tuning is essential since ethylene, produced by the hydrogenation of acetylene within the framework, should have difficulty in migrating out of the framework and entering the product stream (samples where the ethanol absorption is low). Thus, optimum catalyst design must take into account the effects of cation sizes, loadings, and the subtle changes in sorption behavior.

Although the absorption data were useful in demonstrating differences in molecular sieving from one exchanged form to the next, the data do not provide a measure of the catalytic activity of the external surface of the zeolite particles. A figure of merit, FM, was defined as the ratio of hydrogenated acetylene to hydrogenated butadiene under the condition that ethylene passed through the bed essentially unreacted. For the commercially available catalyst under plant conditions, about 60% of the butadiene and all of the acetylene in the feed is hydrogenated, yielding a FM ~1.6.

The initial zeolite catalysts that were prepared exhibited low FM values even though the absorption properties were fine-tuned. This apparent lack of selectivity suggested that the catalytic sites dominating the product spectrum must be located on the surface of the exchanged zeolites. Such metal sites on the external surface are more accessible in comparison to sites within the zeolite framework and can therefore override the contribution to the product spectrum made by the internal sites. The external sites were selectively poisoned by the addition of thiophene to the feed stream. Thiophene is larger than the pore opening of the zeolite; hence it selectively poisoned the metal catalyst on the external surface of the zeolite. Further improvements were realized by using

tetraethylorthosilicate, TEOS, to deposit a silica coating on the external surface of the zeolite. For the samples shown in Table 20, the TEOS treatment improved the catalytic performance but did not alter the sorption data significantly. The TEOS treatment was mild enough such that the size of the zeolite pore openings was not affected. Apparently, the TEOS treatment is able to cover some of the metal catalyst on the external surface of the zeolite that would otherwise not react with thiophene.

Compared to a commercial catalyst which hydrogenates 60% of butadiene and all of the acetylene, the new catalysts totally hydrogenate acetylene with only 10-20% hydrogenation of the butadiene and almost no hydrogenation of ethylene. Thus, to achieve selective hydrogenation, that is, to obtain a product spectrum dominated by catalytic sites within the zeolite framework, poisoning of the metal sites on the external zeolite surface as well as fine-tuned diffusion control are essential.

Table 20. TEOS treatment of Ni,M-A zeolite catalysts.

Catalyst	g absorbed/100g sample			
M	MeOH	EtOH	nPOH	FM
K (Control)	17.0	3.0	0.4	5.9
K + TEOS	17.1	5.0	0.6	9.1
Rb (Control)	15.2	9.2	0.3	7.7
Rb + TEOS	15.1	8.6	0.3	10.0

8.2 COATING EFFECTS

In order to improve absorption selectivity or to inhibit surface reactivity when molecular sieves are used as catalysts or supports, the external surface is sometimes coated or chemically treated as noted above. Although changes in the framework caused by such treatments can be small or undetected, the framework absorption properties can be altered significantly.

In the methylation of toluene, H-ZSM-5 was used as the catalyst. As part of the improved process, an objective was to eliminate the unselective catalysis occurring on the external surface of the crystals. The zeolite was treated with TEOS and a silica coating deposited. The improvement in selectivity was much greater than anticipated but was reasonable after considering the absorption data shown in Table 21. The coating slightly reduced the amount of accessible framework for the readily absorbed hexane and *p*-xylene. But the larger cyclohexane molecule was virtually excluded from entering the framework as were the *o*- and *m*-xylene isomers. Thus, if toluene methylation were to produce either *o*- or *m*-xylenes inside the frameworks, they would be inhibited from exiting the framework because the coating slightly reduced the opening of the surface

Table 21. Effects of TEOS surface treatments of H-ZSM-5 on absorption.

Sample I.D.	g absorbed/100 g sample			*p*-Xyl	0-Hex	*m*-Xylene	*o*-Xylene
	n-Hexane	*p*-Xylene	cyclohexane	n-Hex	n-Hex	®	®
1. Uncoated	9.2	11.9	4.4	1.293	0.478	1.2	1.4
1. Coated	8.8	11.3	0.1	1.284	0.011	0	0
2. Uncoated	11.3	14.3	2.4	1.265	0.212	0.6	0.1
2. Coated	10.6	13.4	0.2	1.264	0.019	0	0
Typical	13.07	15.78	7.38	1.218	0.638		

® absorption values at 20 hours; not equilibrium values.

pores. Thus, the silica coating appears to be bi-functional: it can reduce or eliminate the unselective surface activity while slightly reducing the dimensions of the pores on the surface of the crystals which controls product migration out of the framework.

In a similar fashion, silica coatings were deposited on the external surface of zeolite rho. The results are shown in Table 22; the sample designated EOS-2 had more silica deposited on it compared to EOS-1. The effect of the coatings on the absorption of methanol and ethanol seems to be slight, if any. However, the absorption of the slightly larger n-propanol molecule is significantly affected, both in the packing and rate of filling ratios. These experiments demonstrate that very fine tuning of the sorption process (as well as catalysis) can be achieved by controlled precipitation on molecular sieve surfaces.

Table 23 shows the effects of HCl and $SiCl_4$ treatment of chabazite and zeolite A. $SiCl_4$ is used to modify the silica:alumina ratio and to coat the zeolite with silica. It seems to be a very harsh treatment as the data for both treated zeolites show they lost considerable crystallinity (measured by methanol absorption) during the treatment and material migrated within the zeolite framework further constraining the packing of ethanol. Treatment by HCl seems to be somewhat milder considering that there is less crystallinity lost and the ethanol:methanol ratio is almost unchanged compared to the starting, untreated sample.

Table 22. TEOS treatment of zeolite H-rho.

Sample I.D.	g absorbed/100g sample			EtOH	nPOH	MeOH	EtOH	nPOH
	MeOH	EtOH	nPOH	MeOH	EtOH	3/20	3/20	3/20
Uncoated	23.92	22.04	19.85	0.921	0.901	0.962	0.962	0.817
EOS-1	23.33	20.42	5.33	0.875	0.261	0.975	0.950	0.334
EOS-2	23.85	20.97	1.98	0.879	0.094	0.971	0.956	0.131
Typical	24.00	21.70	20.20	0.923	0.938	0.986	0.962	0.958

Table 23. The effects of HCl and $SiCl_4$ treatment of chabazite and zeolite A.

Sample I.D.	g absorbed/100 g sample			EtOH	nPOH
	MeOH	EtOH	nPOH	MeOH	EtOH
H-Chabazite-1	13.47	12.52	2.65	0.929	0.212
$SiCl_4$-treated	10.71	8.18	1.22	0.764	0.149
H-Chabazite-2	17.88	15.73	1.92	0.880	0.122
HCl-treated	14.02	13.01	1.02	0.928	0.078
5A	20.89	20.30	10.74	0.972	0.529
$SiCl_4$-treated	14.89	11.44	3.67	0.768	0.321

8.3 MIGRATION OF SPECIES WITHIN THE FRAMEWORK

The concept of "molecular traffic control" was first suggested by Derouane and co-workers and was applied to describe absorption phenomena within pentasil zeolites [28]. Essentially, framework structures with intersecting channels can be thought of in macroscopic terms of avenues and streets. A stalled car can impede the flow of traffic just as a large chemisorbed molecule or charge compensating cation might hinder transport down a channel system. A bus making a sharp right turn into a narrow one way street has its equivalence, for example, on the molecular scale, of a dodecane molecule trying to go from the straight channel in ZSM-5 into a sinusoidal one. The effects of molecular traffic control are readily displayed as consequences of reaction selectivity imposed by dual channel framework structures.

In one study, the presence of co-absorbed water had a pronounced effect on migration and catalytic hydrogenation selectivity. The competitive hydrogenation of cyclopentene and 4-methylcyclohexene was catalyzed by zeolites containing rhodium ions [29]. For the nearly dry zeolite Rh-ZSM-11, there was little hydrogenation selectivity for the cyclopentene; this observation agreed with absorption data. However, when water was added to the zeolite prior to the reaction, the selectivity of cyclopentene (vs. cyclohexene) hydrogenation increased significantly as shown in Table 24. Water, which doesn't play a part in the reaction, is absorbed near the Rh-ions (and framework aluminum). At low co-absorbed water contents, the migration of the larger cyclohexene molecule towards the catalytic Rh-site is more affected than that of the smaller cyclopentene molecule; a consequence of Moore and Katzer's correlation of molecular size and diffusion kinetics. Thus, the hydrogenation selectivity increases until a maximum is reached at a specific water content. Above this level of co-absorbed water, migration of both molecules to the catalytic sites is quite impaired and, as a consequence, the hydrogenation selectivity falls off. As expected, the hydrogenation rates are significantly reduced because of the reduced migration (diffusion) rates. A reviewer of that study suggested that the water of hydration was not only surrounding the active Rh sites but also modifying their oxidation

Table 24. The effect of co-absorbed water on the selectivity of the Rh-ZSM-11 catalyzed hydrogenation of cyclopentene/4-methylcyclohexene mixtures.

Weight % Co-Absorbed Water	Hydrogenation Selectivity*
0.54	1.0
1.04	10.6
1.22	11.3
1.81	19.7
2.19	46.9
2.90	22.9
5.10	9.1
8.67	6.2

* Ratio of rate of hydrogenation of cyclopentene/rate of hydrogenation of 4-methylcyclohexene.

states. Several years later, it was unambiguously shown that co-adsorbed water could modify product selectivity without taking part in a reaction.

In this study, it was found that the photochemistry of *o*- and *p*-methylbenzyl benzyl ketones, *o*-A-C(O)-B and *p*-A-C(O)-B, in the presence of pentasil zeolites follows strikingly different pathways due to the location of the adsorbed ketone or the presence of co-absorbed water [30]. The product distribution demonstrated the effects of absorption and diffusion on the radical species produced by photolysis. *p*-A-C(O)-B is readily absorbed within the pentasil framework and produces *p*-AB as the primary product. In contrast, the photolysis product distributions of *o*-A-C(O)-B can be dramatically varied depending upon the extent of its absorption into the framework. By addition of a non-reactive titrant, water, after the ketone adsorption, the photolysis product distributions were systematically varied depending upon the aluminum content of the framework. For high aluminum samples, the addition of co-absorbed water forced the ketone to the external surface of the zeolite which the subsequent photolytic product distribution ably demonstrated. In some cases, the co-absorbed water forces the ketones into the hydrophobic regions of the ZSM-5 framework. The observed product distributions were completely described by considerations of

- the size and shape absorption of the pentasil zeolites.
- the sorption of water by the hydrophilic sites of the pentasil zeolites (which depends upon the framework aluminum content).
- the hydrophobic characteristics of the pentasil channels which do not contain framework aluminum.

Recently, Turro and co-workers showed how the product distributions of chlorination relate to the topology of the ZSM-5 framework and the geometry and location of the absorbed dodecane species [31]. It was observed that the photo-induced chlorination of absorbed n-dodecane selectively occurs at the ends of the chain rather than in the center. The observed selectivity is a function of the loading of the substrate, the nature of the charge compensating cation, and the framework aluminum content. The chlorinating

radicals enter and diffuse into the framework while the target dodecane molecules are absorbed at specific regions within the ZSM-5 framework and are relatively immobile. The product distributions effectively characterize the locations of the absorbed dodecanes as well as the path the radical must have taken.

9. Summary and Conclusions

Absorption of probe molecules of varying geometries and sizes is used to characterize the framework dimensions and topography of molecular sieves. From unit cell dimensions derived from X-ray diffraction and assumptions about the size of the framework forming species, a pore volume can be calculated. The size and chemical behavior of the oxygen in the sieve suggests that the framework bonding is predominantly covalent with a radius 1.5-1.7 Å. The volumes of the absorbed probe molecules, using their liquid densities, are then compared to the calculated pore volume. The constraint on the packing of the absorbed molecules is quantified by comparing their packing density to their density in the liquid state. Further, the packing of probe molecules into the same pore volume is compared via a ratio technique called the 'packing ratio'. The effect of the lattice geometry and framework dimensions on the 'packing ratios' is to provide a set of characteristic values for a given molecular sieve. The combination of X-ray diffraction and absorption measurements permits the crystallinity of a molecular sieve to be quantified. The absorption values and packing ratios for molecular probes into zeolites rho and ZSM-5 are presented as expectation values for other scientists to use as bases of comparison.

Absorption is used to characterize zeolites such as chabazite, A, and ZK-5 as well as ion-exchange effects. The effect of different templates molecules on the absorption properties of ZSM-5 is discussed; the absorption and packing ratios provide sensitive indicators of very small changes in framework dimensions. Also discussed is the application of absorption measurements to understand the effects of surface treatments of zeolite catalysts as well as to provide a better understanding of migration of guest molecules within the pentasil zeolite frameworks.

Acknowledgments

Many of the chapters in this book are written by colleagues with whom the authors had the pleasure of working. In addition, the authors would like to cite these colleagues: Glover Jones for the in-situ X-ray diffraction studies, Ted Gier for the syntheses of rho, George Sonnichsen and Mike Keane for the methylamines reaction data, Gunter Teufer for discussions and X-ray diffraction analyses of the ZSM-5 system, Bob Shannon and Ed Moran for their ZSM-5 preparations, John Parise and Reinhard Fischer for neutron diffraction studies, Cris Bonifaz for acetylene hydrogenation data, Norman Herron and Bill Seidel for olefin hydrogenation data, and our technicians, Brian Arters, Bill Stevens,

Earl Jones, Bob Shiffer, Charlie Perry, Ron Nickle, Walt Weber, Penrose Hollins, and "Chunky" McCartney. DuPont Contribution No. 7102.

References

1. M. Smart, *Chemicals Economics Handbook*, SRI International, (1992).
2. R. Szostak, *Handbook of Molecular Sieves*, Van Nostrand Reinhold, New York (1992).
3. $AlPO_4$-8:
   R. M. Dessau, J. L. Schlenker, and J. B. Higgins, *Zeolites*, **10**, 522 (1990).
   J. W. Richardson, Jr. and E. T. C. Vogt, *Zeolites*, **12**, 13 (1992).
   VPI-5:
   L. B. McCusker, Ch. Baerlocher, E. Jahn, and M. Buelow, *Zeolites*, **11**, 308 (1991).
   M. E. Davis, C. Saldarriaga, C. Montes, J. Garces, and C. Crowder, *Nature* **331**, 698 (1988).
   Cloverite:
   M. Estermann, L. B. McCusker, Ch. Baerlocher, A. Merrouche, and H. Kessler, *Nature*, **352**, 320 (1991).
4. F. Liebau, *Structural Chemistry of Silicates*, Springer-Verlag, Würzburg, p 136 (1985).
5. D. W. Breck, *Zeolite Molecular Sieves*, J. Wiley and Sons, New York, pp 607, 633-41 (1974).
6. R. Szostak, *Molecular Sieves: Principles of Synthesis and Characterization*, Van Nostrand Reinhold, New York (1989).
   H. van Bekkum, E. M. Flanagen, and J. C. Jansen (Eds.), *Introduction to Zeolite Science and Practice*, Elsevier, Amsterdam (1991). (*Stud. Surf. Sci. Catal.*, **58** (1991)).
7. J. E. Huheey, *Inorganic Chemistry*, 2nd Edition, Harper and Row, New York, p 232 (1978).
8. W. M. Meier and D. H. Olson, *Atlas of Zeolite Structure Types*, Third Edition, Butterworth-Heinemann, Boston, p 9 (1992).
9. S. G. Hill and D. Seddon, *Zeolites*, **5**, 173 (1985).
10. W. W. Kaeding, C. Chu, L. B. Young, B. Weinstein, and S. A. Butter, *J. Catal.* **67**, 159 (1981).
    J. Koresh and A. Soffer, *J. Chem. Soc., Faraday I*, **76**, 2457 (1980).
    J. Koresh and A. Soffer, *J. Chem. Soc., Faraday I*, **76**, 2472 (1980).
    R. M. Moore and J. R. Katzer, A. *I. Ch. E. Journal*, **18**, 816 (1972).
11. Fisher Scientific Co., Cat. No. 12-824, *U.S. Patent 2,308,402* (1940).
12. L. Gurvitsch, *Russ. J. Phys. Chem.*, **47**, 805 (1915).
13. These references should provide a reasonable overview of sorption:
    See [5], Chap. 8, "Adsorption by Dehydrated Zeolite Crystals", p 593ff.

S. J. Gregg and K. S. W. Sing, Chap. 4, Adsorption of Gases on Porous Solids, *Surface & Colloid Science*, **19**, 231 (1976).
J. Koresh, *J. Colloid Interface Science*, **88**, 398 (1982).
J. L. Soto, P. W. Fisher, A. J. Glessner, and A. L. Myers, *J. Chem. Soc., Faraday I*, **77**, 157 (1981).
A. P. Vavlitis, D. M. Ruthven, and K. F. Loughlin, *J. Colloid Interface Science*, **84**, 526 (1981).
The titles of these papers are included to show the diversity of studies:
"Sorption and Diffusion of Gaseous Hydrocarbons in Synthetic Mordenite", C. N. Satterfield and A. J. Frabetti Jr., *A. I. Ch. E. Journal*, **13**, 731 (1967).
"Desorption and Counterdiffusion Behavior of Benzene and Cumene in H-Mordenite", C. N. Satterfield, J. R. Katzer, and W. R. Vieth, *Ind. Eng. Chem. Fundam.*, **10**, 478 (1971).
"Restricted Diffusion in Liquids within Fine Pores", C. N. Satterfield, C. K. Colton, and W. H. Pitcher, *A. I. Ch. E. Journal*, **19**, 628 (1973).
"Sorption and Diffusion Properties of Natural Zeolites", Y. H. Ma and T. Y. Lee, in *Natural Zeolites*, L. B. Sand and F. A. Mumpton (Eds), Pergamon Press, Elmsford, New York, p 373 (1976).
"Interpretation and Correlation of Zeolite Diffusivities Obtained from NMR and Sorption Experiments", J. Karger and J. Caro, *J. Chem. Soc., Faraday I*, **73**, 1363 (1977).
"Mass Transport in Heterogenenous Catalysts", J. C. Vedrine, in *Mass Transport in Solids*, F. Beniere and R. A. Catlow (Eds), Plenum, New York, Chap. 20 (1981).
"Kinetics of Nonisothermal Sorption: Systems with Bed Diffusion Control", D. M. Ruthven and L. -K. Lee, *A. I. Ch. E. Journal*, **27**, 654 (1981).
"Diffusion in Zeolites", J. Karger and D. M. Ruthven, *J. Chem. Soc., Faraday I*, **77**, 1485 (1981).
"Diffusion-Controlled Adsorption Kinetics. General Solution and Some Applications", K. J. Mysels, *J. Phys. Chem.*, **86**, 4648 (1982).
"Interpretation of Sorption and Diffusion Data in Porous Solids", R. Aris, *Ind. Eng. Chem. Fundam.*, **22**, 150 (1983).
"Adsorption and Diffusion of Gases in Zeolites", L. V. C. Rees, *Chemistry and Industry (London)*, 252 (1984).
"Nonisothermal Sorption Kinetics in Porous Adsorbents", R. Haul and H. Stremming, *J. Colloid Interface Science*, **97**, 348 (1984).
14. R. M. Moore and J. R. Katzer, *A. I. Ch. E. Journal*, **18**, 816 (1972).
15. L. Abrams and D. R. Corbin, *J. Catal.*, **127**, 9 (1991).
16. L. Abrams, M. Keane, and G. C. Sonnichsen, *J. Catal.*, **115**, 361 (1989).
17. J. B. Parise, L. Abrams, T. E. Gier, D. R. Corbin, J. D. Jorgensen, and E. Prince, *J. Phys. Chem.*, **88**, 2303 (1984).
18. L. Abrams, D. R. Corbin, and M. Keane, *J. Catal.*, **126**, 610 (1990).

19. D. H. Olson, G. T. Kokotailo, S. L. Lawton, and W. M. Meier, *J. Phys. Chem.*, **85**, 2238 (1981).
20. E. G. Derouane and Z. Gabelica, *J. Catal.*, **65**, 486 (1980).
E. M. Flanigen, J. M. Bennett, R. W. Grose, J. P. Cohen, R. L. Patton, R. M. Kirchner, and J. V. Smith, *Nature*, **271**, 512 (1978).
A. Auroux, H. Dexpert, C. LeClercq, and J. Vedrine, *Appl. Catal.*, **6**, 95 (1983). C. G. Pope, *J. Catal.*, **72**, 174 (1981).
H.-J. Doelle, J. Heering, L. Rickert, and L. Marosi, *J. Catal.*, **71**, 27 (1981).
R. LeVanMao, O. Pilati, A. Marzi, G. Leofanti, A. Villa, and V. Ragaini, *React. Kinet. Catal. Lett.*, **15**, 293 (1980).
H. Nakamoto and H. Takahashi, *Zeolites*, **2**, 67 (1982).
21. A comparison of the relative diffusion coefficients was made by using a modified form of the Crank equation: $(Q_t-Q_o)/(Q_{eq}-Q_o) = c*(Dt)^{1/2}$, {[5] p. 673}where Q_t is the amount sorbed at time t, Q_{eq} is the equilibrium amount, c is a constant depending on the geometry of the crystals, and D is the diffusion coefficient. For the case where Q_o is zero, the ratio of Q_t to Q_{eq} is the occupancy of the crystals. Rearranging the equation yields: $D = (k/t)*(Q_t/Q_{eq})^2$, which is valid only for short times.
22. Z. Gabelica, J. B. Nagy, and G. Debras, *J. Catal.*, **84**, 256 (1983).
23. E. G. Derouane, S. Detremmerie, Z. Gabelica, and N. Blom, *Appl. Catal.*, **1**, 201 (1981).
24. P. A. Jacobs, E. G. Derouane, and J. Weitkamp, *J. Chem. Soc., Chem. Commun.*, 592 (1981).
25. S. M. Csicsery, *Zeolites*, **4**, 202 (1984).
26. V. N. Ramannikov, A. S. Loktev, A. N. Spektor, G. L. Bitman, K. G. Ione, P. S. Chekrii, *Neftekhimiya*, **31**, 409-15 (1991).
27. D. R. Corbin, L. Abrams, and C. Bonifaz, *J. Catal.*, **115**, 420 (1989).
28. E. G. Derouane, P. Dejaifve, Z. Gabelica, and J. Vedrine, *J. Chem. Soc., Faraday Disc.*, **72**, 331 (1981).
E. G. Derouane, *J. Catal.*, **72**, 177 (1981).
29. D. R. Corbin, W. C. Seidel, L. Abrams, N. Herron, G. D. Stucky, and C. A. Tolman, *Inorg. Chem.*, **24**, 1800 (1985).
30. N. J. Turro, C. -C. Cheng, L. Abrams, and D. R. Corbin, *J. Am. Chem. Soc.*, **109**, 2449 (1987).
31. N. J. Turro, N. Han, X-G. Lei, J. R. Fehlner, and L. Abrams, *J. Am. Chem. Soc.*, (submitted).

Abstract. Molecular sieves are inorganic framework structures generally composed of crystalline aluminosilicate tetrahedra which are arranged to form channels of 2-10 Å diameters and cages with dimensions from 6-15 Å. Absorption of probe molecules of varying geometries and sizes is used to characterize the framework dimensions and topography in concert with X-ray diffraction identification of the specific structure. From unit cell dimensions and assumptions about the size of the framework forming species, a pore volume can be calculated. The volumes of the absorbed probe molecules, using their liquid densities, are then compared to the calculated pore volume. The constraint on the packing of the absorbed molecules is quantified by comparing their packing density to their density in the liquid state. Further, the packing of different probe molecules into the same pore volume is compared via a ratio technique called the 'packing ratio'. The effect of the lattice geometry and framework dimensions on the 'packing ratios' is to provide a set of characteristic values for a given molecular sieve. The packing ratios for zeolites rho and ZSM-5 are presented as expectation values for other scientists to use as bases of comparison.